APTD-0621

APTD-0621

PB196749

RESEARCH REPORT

BATTELLE MEMORIAL INSTITUTE

COLUMBUS LABORATORIES

Reproduced by
NATIONAL TECHNICAL
INFORMATION SERVICE
Springfield, Va. 22151

16

SUMMARY REPORT

on

INVESTIGATION OF THE REACTIVITY OF LIMESTONE AND DOLOMITE FOR CAPTURING SO_2 FROM FLUE GAS

to

NATIONAL AIR POLLUTION
CONTROL ADMINISTRATION

November 20, 1970

by

R. W. Coutant, R. E. Barrett, R. Simon,
B. E. Campbell, and E. H. Lougher

BATTELLE MEMORIAL INSTITUTE
Columbus Laboratories
505 King Avenue
Columbus, Ohio 43201

Battelle Memorial Institute · COLUMBUS LABORATORIES

505 KING AVENUE COLUMBUS, OHIO 43201 · AREA CODE 614, TELEPHONE 299-3151 · CABLE ADDRESS: BATMIN

November 20, 1970

Mr. Robert H. Borgwardt
Division of Process Control Engineering
National Air Pollution Control Administration
3914 Virginia Avenue
Cincinnati, Ohio 45227

Dear Mr. Borgwardt:

Contract No. PH 86-67-115

Enclosed are 75 copies plus one reproducible copy of our summary report on your program "Investigation of the Reactivity of Limestone and Dolomite for Capturing SO_2 from Flue Gas". This report covers work done on this program between May 29, 1969, and October 30, 1970.

We will welcome your comments on the report and on the research.

Very truly yours,

R. W. Coutant
Associate Chief
Atmospheric Chemistry and
Combustion Systems Division

RWC:ao

Enc.

STANDARD TITLE PAGE FOR TECHNICAL REPORTS	1. Report No. APTD-0621	2. Gov't Accession No.	3. Recipient's Catalog No.
4. Title and Subtitle: Investigation of the Reactivity of Limestone and Dolomite for Capturing SO_2 from Flue Gas			5. Report Date: November 1970 6. Performing Organization Code
7. Author(s): R. W. Coutant, et al.			8. Performing Organization Rept. No.
9. Performing Organization Name and Address: Battelle Memorial Institute, Columbus Laboratories, 505 King Avenue, Columbus, Ohio 43201			10. Project/Task/Work Unit No. 11. Contract/Grant No. PH 86-67-115
12. Sponsoring Agency Name and Address: Division of Process Control Engineering, National Air Pollution Control Administration, 3914 Virginia Avenue, Cincinnati, Ohio 45227			13. Type of Report & Period Covered 14. Sponsoring Agency Code

15. Supplementary Notes

16. Abstracts

Improved experimental equipment and analytical techniques have enabled more detailed study of the reaction between Limestone 2061 and SO2 in flue gas. Progress was made in analysis of results and development of techniques for prediction of performance of the process in a boiler by means of both empirical and theoretical evaluation of various aspects of the process. Results obtained for Limestone 2061 indicate: (1) maximum reactivity at injection temperatures not exceeding about 2200 F, (2) reduced sorption efficiency at low SO2 concentration, (3) possible improvement in the efficiency of the process at excess oxygen levels above 3 percent, and (4) reduced efficiency as a result of use of precalcined stone.

17. Key Words and Document Analysis. (a). Descriptors

Air pollution control equipment
Sulfur dioxide
Flue gases
Limestone
Laboratory equipment
Chemical analysis
Boilers
Temperature
Combustion
Chemical reactions
Rocks

17b. Identifiers/Open-Ended Terms

17c. COSATI Field/Group 13/02, 07/01

18. Distribution Statement	19. Security Class (This Report)	21. No. of Pages
Unlimited	UNCLASSIFIED	75
	20. Security Class. (This Page) UNCLASSIFIED	22. Price

FORM NBS-867(1-70)

This report was furnished to the Air Pollution Control Office by the Battelle Memorial Institute in fulfillment of Contract No. PH 86-67-115.

TABLE OF CONTENTS

	Page
INTRODUCTION	1
SUMMARY	1
Experimental Work	1
Conclusions and Recommendations	2
EQUIPMENT AND MATERIALS	3
The Dispersed-Phase Reactor	3
Auxiliary Systems	6
Cooling Systems	6
Monitoring Equipment	6
Probes	6
Temperature and Time Profiles	9
Materials Preparation and Analysis	9
Particle Sizing	9
Chemical Analyses	11
EXPERIMENTAL WORK AND DISCUSSION	13
Reaction of Limestone with SO_2	13
Effect of Temperature	16
Alternative Correlation Procedures	20
Effect of SO_2 Concentration	22
Effect of Oxygen Concentration	22
Effect of Precalcination of Stone	28
Importance of Sulfite Formation	28
Calcination of Limestone	32
Basis of Representation	32
Model of Calcination Process	32
Effect of Porosity on Thermal Conductivity	35
Experimental Studies	37
Effect of Gas Temperature	37
FUTURE WORK	45
REFERENCES	46
APPENDIX A	
REACTOR DATA	A-1
APPENDIX B	
COMPUTER PROGRAM - SULFEX (PROCESSING OF ANALYTICAL DATA)	B-1
APPENDIX C	
COMPUTER PROGRAM - DRH2 (DATA CORRELATION)	C-1
APPENDIX D	
COMPUTER PROGRAM - CALCIN (CALCINATION MODEL)	D-1

LIST OF FIGURES

		Page
Figure 1.	Dispersed-Phase Reactor	4
Figure 2.	Reactor Configuration	5
Figure 3.	The 400 F (Dow Therm) Coolant System	7
Figure 4.	The 160 F (Mineral Oil) Coolant System	8
Figure 5.	Temperature Profile in Dispersed-Phase Reactor	10
Figure 6.	Effect of SO_2 on Calcination.	14
Figure 7.	Effect of Temperature on SO_2 Reaction	15
Figure 8.	Effect of Temperature on Reaction Rate.	17
Figure 9.	Comparison of Reactor with Shawnee Boiler--Time-Temperature Profile.	19
Figure 10.	Effect of SO_2 Concentration on Reactivity	24
Figure 11.	Dependence of Sulfation Rate on SO_2 Concentration at Various Sulfate Loadings.	25
Figure 12.	Effect of O_2 Concentration on Reactivity	26
Figure 13.	Dependence of Reaction Rate on O_2 Concentration at Various Sulfate Loadings.	27
Figure 14.	Calciner--Injector.	29
Figure 15.	Runs Made With Precalcined Stone.	30
Figure 16.	Relation of Sulfite Content to Degree of Calcination.	31
Figure 17.	Partly Calcined Spherical Limestone Particle.	32
Figure 18.	Model of a Porous Solid	36
Figure 19.	Effective Thermal Conductivity of CO_2-Filled Lime	37
Figure 20.	Calcination of -270+325-Mesh Limestone at 1770 F.	38
Figure 21.	Calcination of -140+200-Mesh Limestone at 1863 F	39
Figure 22.	Calcination of -140+200-Mesh Limestone at 1600 F	40
Figure 23.	Calcination of -140+200-Mesh Limestone at 1770 F	41

LIST OF FIGURES
(Continued)

Page

Figure 24. Calcination of -140+200-Mesh Limestone at 2068 F . . 42

Figure 25. Apparent Activation Energy for Calcination. 43

Figure 26. Effect of Pore Size on Calcination Rate 44

LIST OF TABLES

Table 1. Data Correlation. 16

Table 2. Apparent Order of Reaction With Respect to SO_2. 23

Table A1. Reactor Data. A-1

Table A2. Reactor Data-Sulfurization. A-2

MANAGEMENT SUMMARY

Improved experimental equipment and analytical techniques have enabled more detailed study of the reaction between Limestone 2061 and SO_2 in flue gas during this contract period of June 27, 1969, through August, 1970. Progress has been made in analysis of results and development of techniques for prediction of performance of the process in a boiler by means of both empirical and theoretical evaluation of various aspects of the process. Results obtained for Limestone 2061 during this period indicate: (1) maximum reactivity at injection temperatures not exceeding about 2200 F, (2) reduced sorption efficiency at low SO_2 concentration, (3) possible improvement in the efficiency of the process at excess oxygen levels above 3 percent, and (4) reduced efficiency as a result of use of precalcined stone. Plans for future work include further development of methods for extrapolation from dispersed-phase reactor results to boiler performance, and further study of the physical and mineralogical properties of various stones in an attempt to develop models for the prediction of stone performance on the basis of these properties.

INVESTIGATION OF THE REACTIVITY OF LIMESTONE AND DOLOMITE FOR CAPTURING SO_2 FROM FLUE GAS

by

R. W. Coutant, R. E. Barrett, R. Simon,
B. E. Campbell, and E. H. Lougher

INTRODUCTION

One of the major air pollutants in the United States is sulfur dioxide produced by burning of fuels containing sulfur. As a part of a national program to develop air-pollution-control processes, the National Air Pollution Control Administration is supporting research on various processes including dry-limestone injection, wet-scrubbing, and molten-carbonate scrubbing. Of the various processes being considered, the dry-limestone injection process is the simplest and most direct, and holds promise for being the easiest process to apply in existing power plants.

The current investigation, conducted under Contract No. PH 86-67-115 was concerned with a study of some of the fundamental aspects of the reactivity of SO2 with limestone. The object of this research was to investigate the kinetics of the reaction of limestone with SO_2 under conditions that simulate those expected in normal power-plant operation. In particular, the course of reaction was studied with respect to calcination of stone, sulfite formation, and sulfate formation under nonisothermal conditions at short residence times (0.1 to several seconds) with injection temperatures ranging from 1600 to about 2450 F.

The ultimate goal of this work is to develop a better understanding of the reactions on which the process is based, and to relate the results of this work to the full-scale demonstration tests of the dry-limestone-injection process being carried out at the Shawnee TVA Steam Plant. In order to facilitate such comparison, the same stone has been used in the laboratory work as that being employed in the Shawnee tests.

SUMMARY

Experimental Work

During this contract period, a new, improved, dispersed-phase reactor was constructed. This new reactor has permitted study of the SO_2-limestone reaction over a wider range of temperature and residence time than was previously possible. Injection temperatures with the new reactor ranged from about 1600 to 2450 F and residence times ranged from < 0.1 to several seconds. Analysis of the results and modeling of the overall reaction to provide a basis for prediction

of process performance in a real boiler has progressed on two fronts: (1) empirical analysis of the data, and (2) theoretical treatment of the process based on heat and mass transport.

Results obtained for the SO_2-limestone reaction, using -140 + 200-mesh stone No. 6061, at mean gas temperatures between 1600 and 2148 F showed a regular increase in both rate of reaction and overall reactivity up to about 1900 to 2000 F, but both rate and overall reactivity declined at higher mean gas temperatures. One obvious explanation for this decline in reactivity at higher temperatures is that the limit of thermal stability of calcium sulfate was approached in these experiments. Also, it was observed that the reaction between SO_2 and limestone commenced immediately upon injection of stone into the reactor, suggesting a direct reaction between SO_2 and $CaCO_3$ without the need for calcination of the stone.

The effect of SO_2 concentration on reactivity at 1700 F was studied with SO_2 concentrations between 500 and 9500 ppm. The results showed an apparent linear relationship between the initial rate of reaction and the square root of the SO_2 concentration. However, at significant sulfate loadings, the rate of reaction is more dependent on SO_2 concentration.

An exploratory study of the effect of oxygen concentration on the SO_2-limestone reaction at 1700 F indicated an augmentation of initial reaction rates at O_2 levels above 3 percent, i.e., 15 percent excess air, but lesser effect at lower O_2 concentrations. However, at significant sulfate loadings, the reaction rates were increased by additional O_2 throughout the range of O_2 concentrations employed.

A study of the effect of partial precalcination of stone on the SO_2-reaction indicated a relatively high initial rate of reaction, but the overall reactivity of the precalcined material was less than that of the raw stone.

Theoretical modeling of the reaction was initiated with development of a procedure for calculation of calcination rates based on non-steady-state heat and mass transfer within the particles of stone. Results obtained with this model are in reasonably good agreement with experimental work carried out during this period, and further development of the model with respect to sorption of SO_2 seems justified.

Conclusions and Recommendations

The results of this investigation of the reactivity of stone No. 2061 suggest that: (1) the injection temperature in a boiler should not be higher than 2000 to 2200 F; (2) the initial rate of reaction is dependent on the square root of the SO_2 concentration, but as the sulfate loading increases, the rate becomes more dependent on SO_2 concentration. This would indicate that the process may function relatively efficiently where SO_2 levels are initially high, but with medium- to low-sulfur fuels, the relative efficiency of the process probably

will be low; (3) it may be possible to improve the efficiency of the process by use of higher excess-air levels in the boiler, although it is recognized that this will decrease boiler efficiency; and (4) the use of precalcined stone in the boiler is not recommended.

EQUIPMENT AND MATERIALS

The Dispersed-Phase Reactor

As pointed out in the Summary Report[(1)]* for the previous contract period, the overall reaction between limestone and SO_2 follows a complex path, the nature of which is, in part, due to the relatively slow heat-up of the stone, resulting from the thermal requirements for calcination. Because of this complex nature, a more detailed study of the reaction was required for a better understanding of the dry-limestone-injection process.

A new dispersed-phase reactor was designed and constructed to conduct the work needed to better define the process. This reactor is of improved design and allows for study of the reaction over a wider range of temperatures and residence times than was possible with earlier versions of the reactor. Also, improvements were made in auxiliary equipment to permit both easier and more flexible operation of the overall system.

Figure 1 is a photograph of the new reactor system, with various parts of the system labeled. A sketch showing the configuration of the main body of the reactor is presented in Figure 2. The reactor is basically a vertical tube with a gas-fired burner at the bottom. Particles of stone or lime are injected through any of a series of ports in the wall, carried upward by the flue-gas stream, and extracted through another port. The residence time of the particles is determined by the probe spacing and the gas velocity. The samples are small compared with the amount of gas to which they are exposed, so that the particles encounter an essentially constant SO_2 concentration throughout the reaction period, there being, on the average, 1 to 2 particles per cubic foot of flue gas. Current results therefore probably do not reflect the influence of dispersion efficiency on SO_2 removal. This fact may well be important in comparing reactor results with those obtained in a boiler. Dispersion of limestone particles in a boiler may not be achieved so readily as in the reactor. Furthermore, in the more dense clouds of particles needed to achieve significant reduction in SO_2 concentration in a boiler, it is expected that the effective mass transport to individual particles may be reduced as a result of the proximity of other particles.** Such interparticle

---

* References are at the end of the report.

** See, for example, Zenz, F. A. and Othmer, D. F., Fluidization and Fluid Particle Systems, Rheinhold Publishing Corp., New York (1960), pp 421-425.

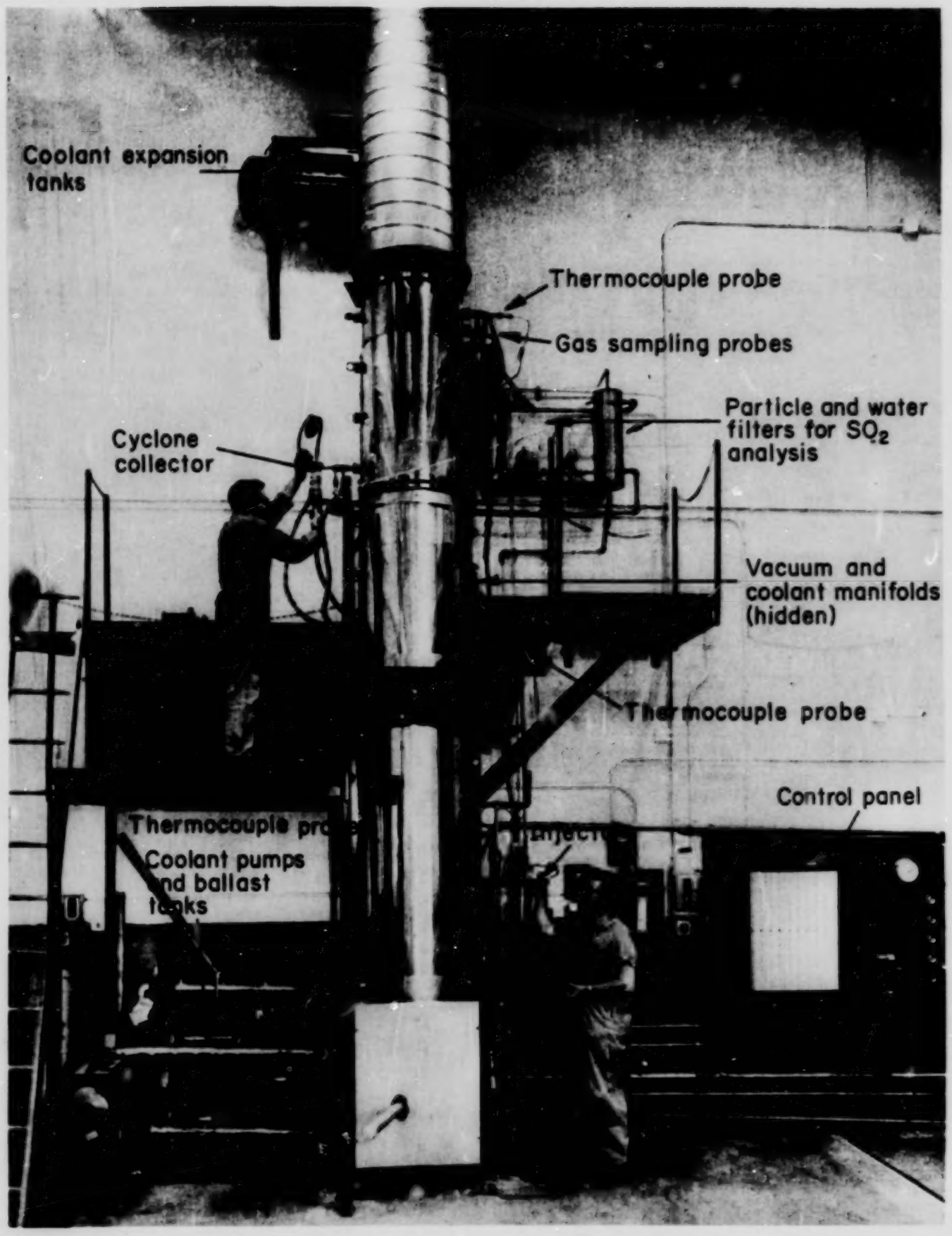

FIGURE 1. DISPERSED-PHASE REACTOR

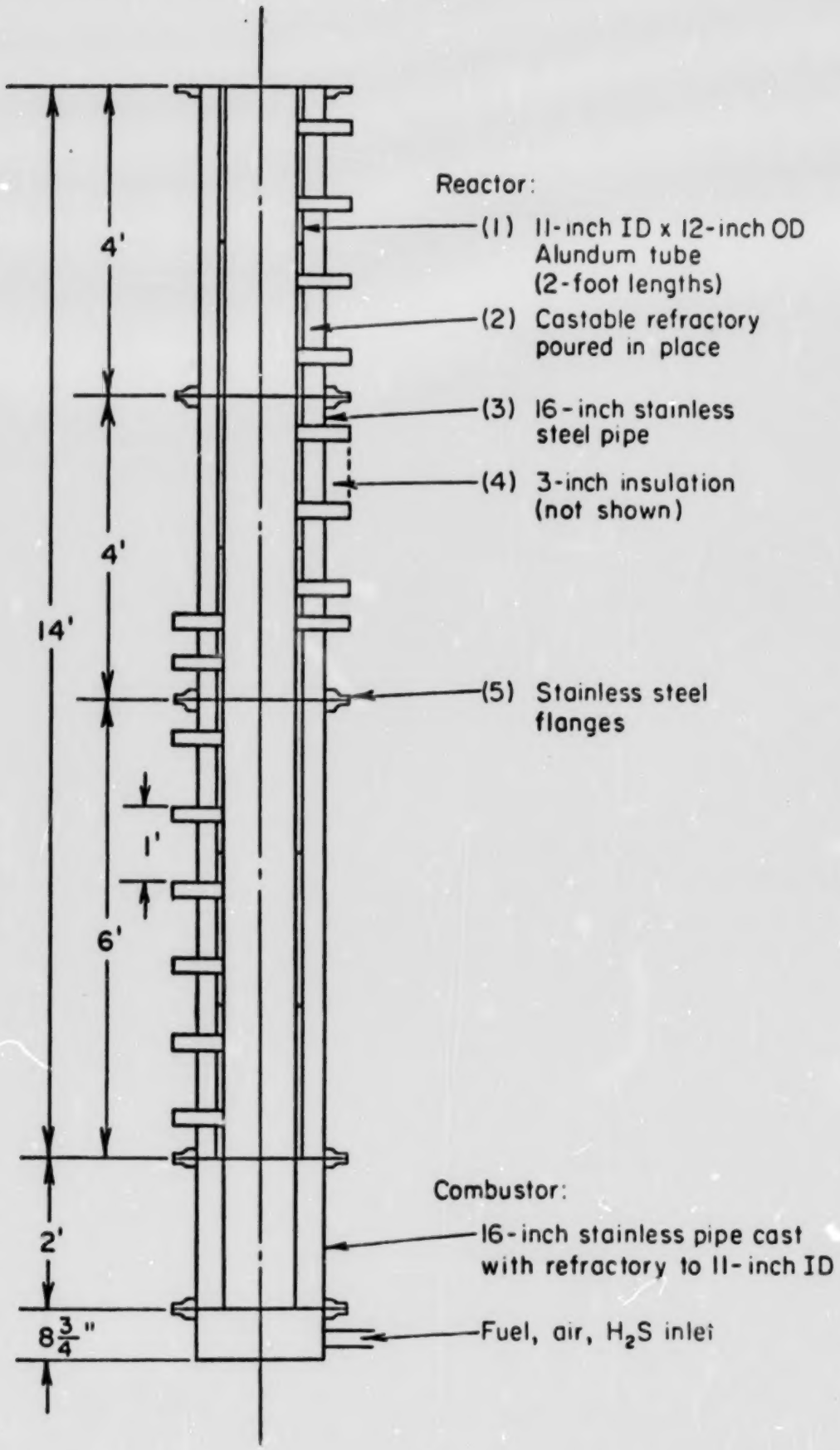

FIGURE 2. REACTOR CONFIGURATION

effects on the mass-transport process are not expected in the "thin" clouds of particles in the reactor. In essence, this means that mass-transport coefficients may be somewhat higher in the reactor than in a boiler.

Auxiliary Systems

All ports and auxiliary equipment for the new reactor are easily accessible either from ground level or from platforms. Multiple-tap manifolds are utilized for the coolant systems and vacuum lines so that probes can be relocated easily and rapidly during a run. Continuous readout equipment for analysis of O_2 and SO_2 and for temperature measurement is located at ground level for convenient monitoring of operating parameters. In general, the physical layout of the new reactor provides for more efficient operation of the system.

Cooling Systems. Two independent cooling systems were used to provide increased flexibility and capacity in controlling temperatures in the system. Schematic representations of these coolant systems are presented in Figures 3 and 4. One system, with Dowtherm as the heat-transfer fluid, was used to maintain the various gas- and particle-sampling probes at about 400 F so that SO_3 would not condense in the probes. The same system was also used to cool the burner plate to prevent flashback of the flame to the plenum below the plate. Thermal balance in the Dowtherm system was achieved with a thermostatted heater and a manually operated, water-cooled heat exchanger.

In the second coolant system, mineral oil at about 160 F was used as the heat-transfer fluid. This system was used to cool the particle-injection probe and the condenser on the SO_3-analysis probe.

Monitoring Equipment. Although Orsat analyses and titration procedures, because of their accuracy and reliability, were used for accurate chemical analysis, continuous monitoring of oxygen and SO_2 also was provided, using a Beckmann Model 315 nondispersive IR analyzer for SO_2 analysis and a Bailey gas analyzer to monitor the oxygen content of the flue gas.

Continuous monitoring of temperatures throughout the reactor system was provided by a 24-point recorder. Gas temperatures at the top, middle, and bottom of the reactor were recorded to provide a continuous record of vertical temperature gradients. Also, wall temperatures at several points in the reactor were recorded. In general, wall temperatures were 100 to 200 F lower than the centerline gas temperatures.

Probes. Gas- and particle-sampling probes were operated from a vacuum source employing a steam ejector. As with the coolant systems, the vacuum system was laid out from a central manifold.

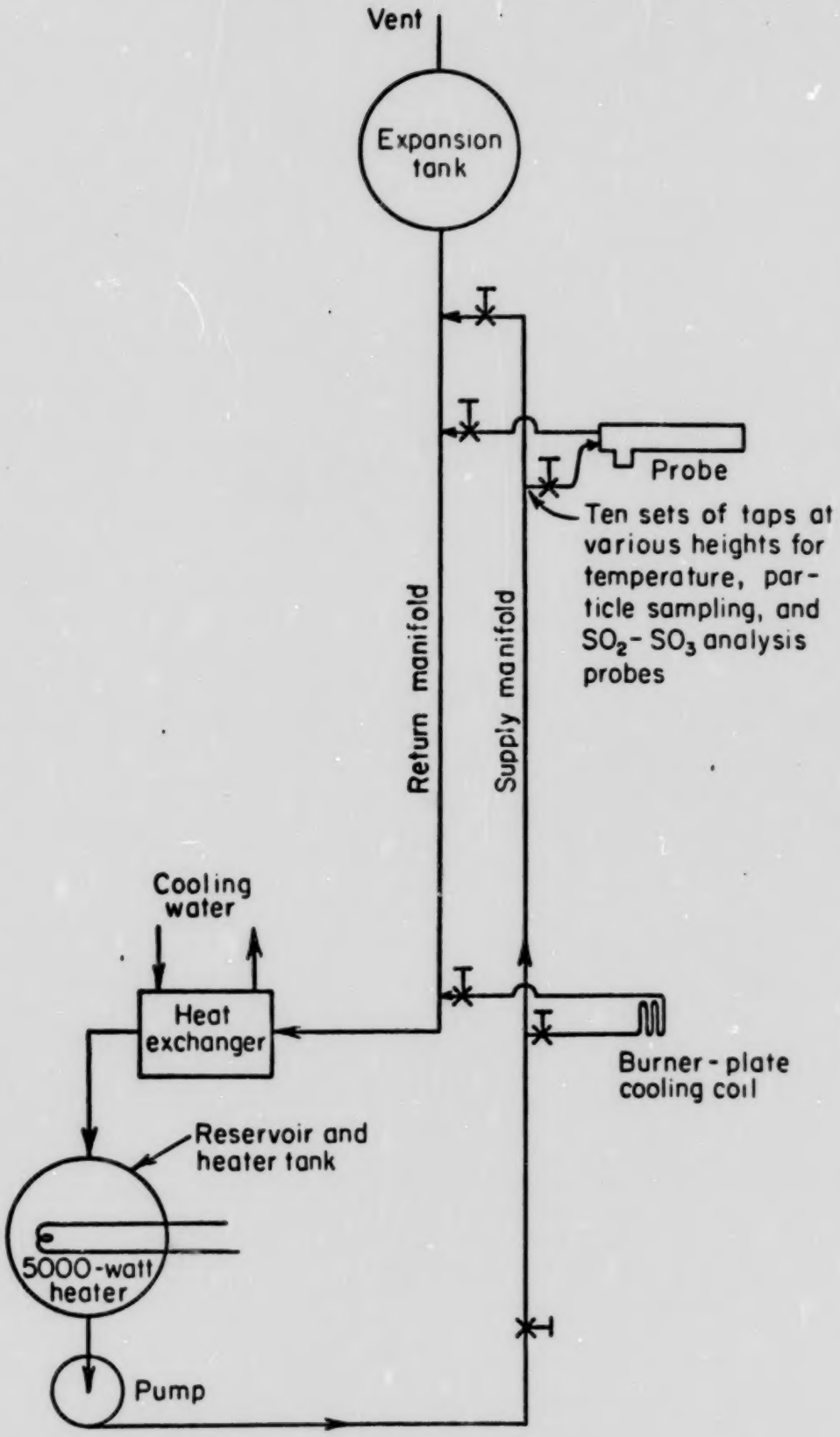

FIGURE 3. THE 400 F (DOWTHERM) COOLANT SYSTEM

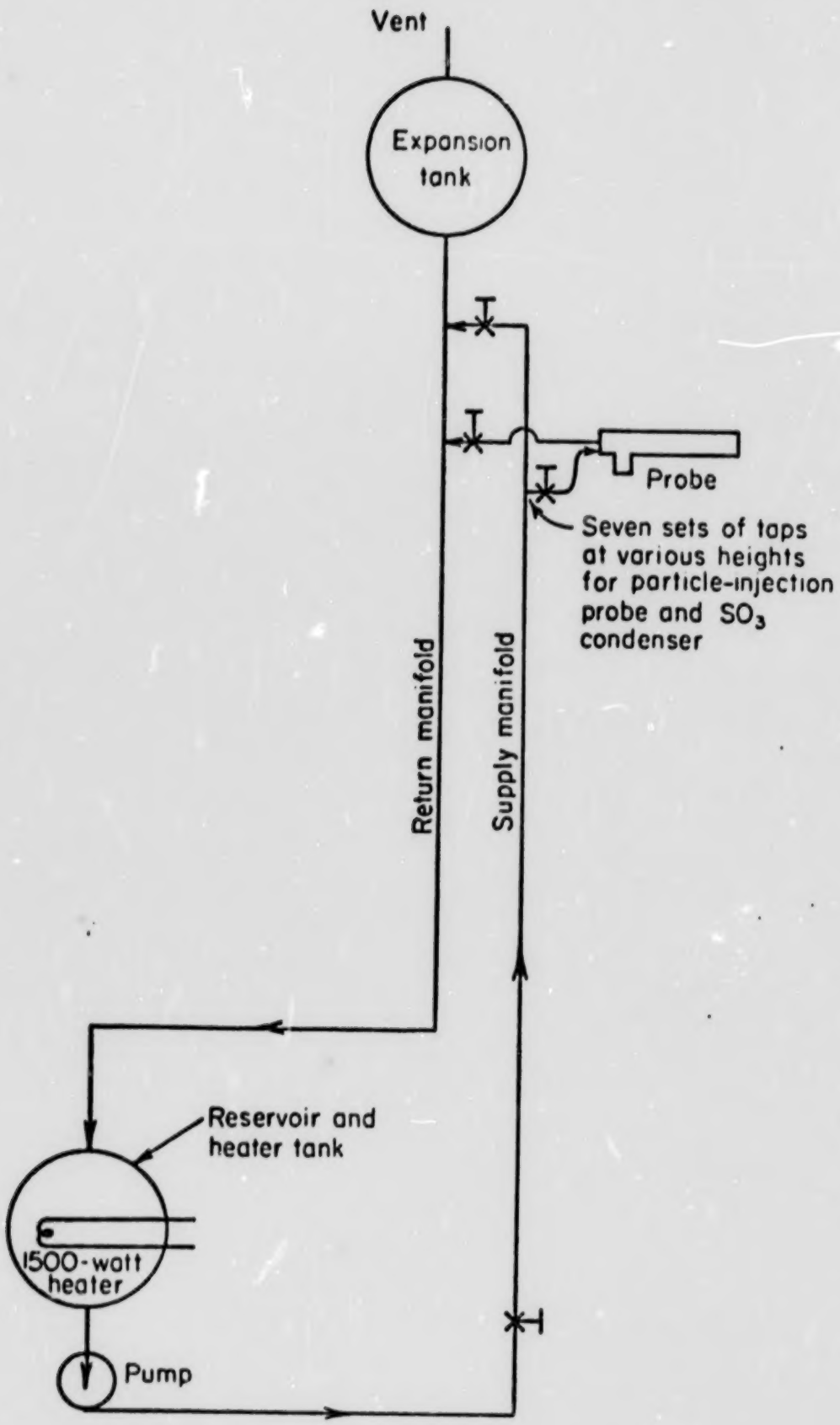

FIGURE 4. THE 160 F (MINERAL OIL) COOLANT SYSTEM

The bottom temperature probe was also used in connection with a safety device. If the temperature at the bottom probe dropped below its point of normal operation, say because of flashback or reduction in gas pressure, the natural-gas feed was automatically shut off. This permitted extended periods of unattended operation so that reactor temperatures could be stabilized during non working hours. Thus, little time was wasted in changing from one operation temperature to another.

Although most of the probes used with the new reactor were essentially of the same design as those employed previously,(1) use of the thimble-filter sampling device was discontinued. With the thimble-filter collector, flue gas was passed over the collected particles continuously during the time needed to collect sufficient sample for analysis. Tests indicated that relatively little of the total sulfurization of the lime occurred in the thimble, but some question still existed concerning the absolute accuracy of the results, and reproducibility of results was not as good as might be hoped. Also, manipulation of the thimble-type collector was awkward and time consuming. Consequently, a cyclone collector was used with the new reactor. This device is simple to use, and samples were collected directly in glass vials for storage prior to analysis.

Temperature and Time Profiles

A typical temperature profile along and normal to the axis of the new reactor is shown in Figure 5. The data indicate a relatively flat temperature profile over the cross section of the reactor and a nearly constant longitudinal gradient. The gradient does depend somewhat on the mean operating temperature of the reactor, with values of 42 and 50 F/ft being obtained at mean temperatures of 1600 and 2050 F, respectively.

Velocity gradients along the reactor also were measured to permit accurate determination of the residence time of particles in the reactor. Measurements indicated that the flow profile was nearly flat over the reactor cross section, with the peak velocity being only about 5 percent greater than the mean velocity. In making calculations of residence time, both the known temperature gradient and the flow profile were taken into account.

Materials Preparation and Analysis

Particle Sizing

Limestone 2061 was used in this study, mostly -140 + 200 U. S. Standard mesh (74 to 105 microns) obtained by grinding and sieving bulk samples provided by NAPCA. In one calcination run, a second size, -270 + 325 U. S. Standard mesh (44-53 microns), was used.

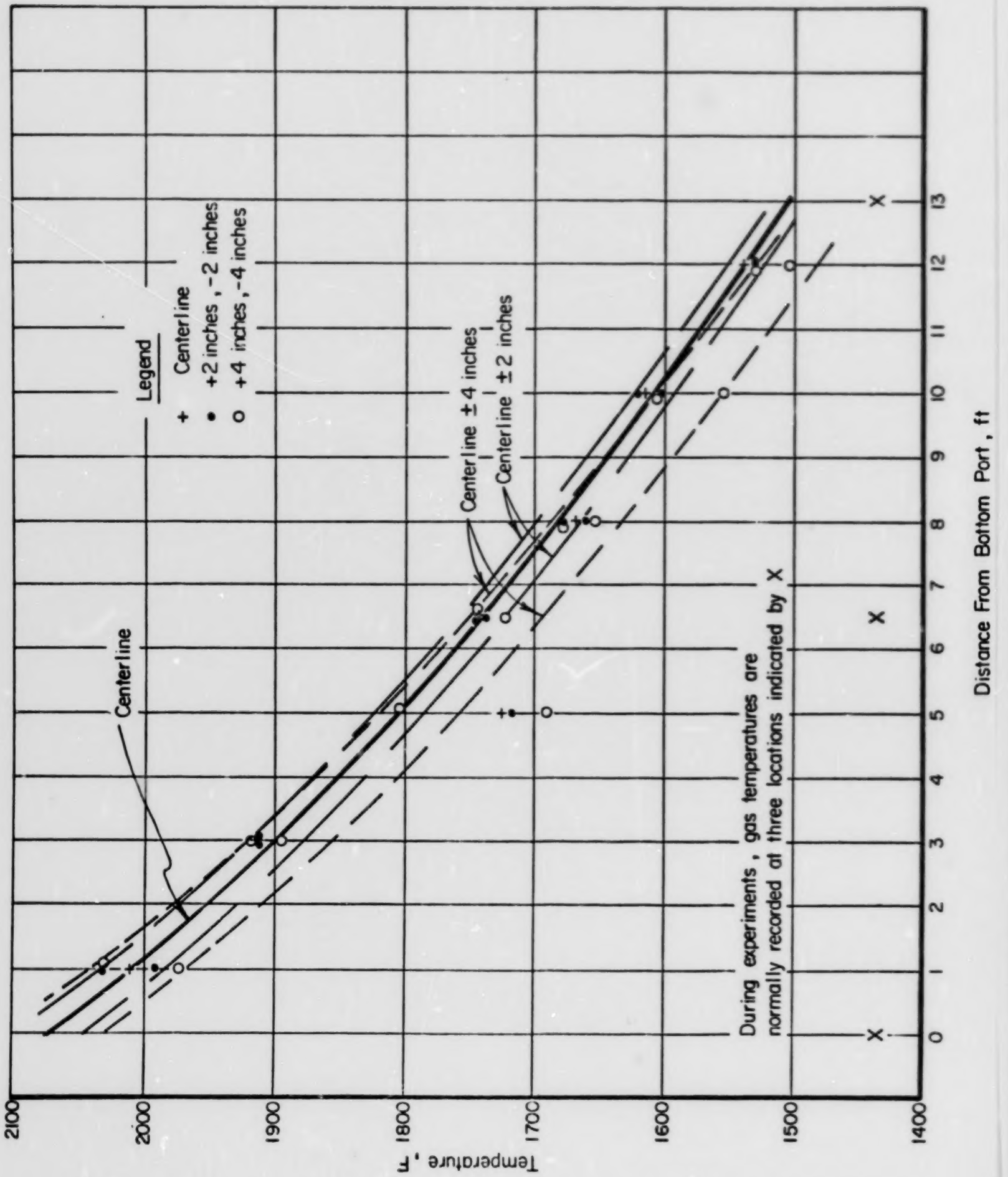

FIGURE 5. TEMPERATURE PROFILE IN DISPERSED-PHASE REACTOR

Chemical Analyses

Samples of -140 + 200-mesh stone were analyzed by atomic-absorption spectrometry and thermogravimetric analysis, and were found to contain appreciably different quantities of calcium, magnesium, and carbonate than those indicated by the analyses provided by Bituminous Coal Research, Inc. Presumably, the samples used came from a different section of the limestone quarry, and hence had a different composition than the samples originally analyzed by BCR.* Samples used in this study showed 41.5 percent loss on ignition, and the resultant lime contained 0.61 percent magnesia and 90.17 percent calcia. Determination of the density of the stone by a water-displacement method indicated a density of 2.58 g/cc (161 lb/ft^3).

Reacted samples obtained from the dispersed-phase reactor were assumed to be composed of

(1) $CaCO_3$, CaO, and unreactive material for the calcination runs

(2) $CaCO_3$, CaO, $CaSO_3$, $CaSO_4$, and unreactive material for the sulfurization runs.

From the analyses given above, the amount of unreactive material in a given sample was 10.9 percent of the total calcium content of the sample expressed as CaO.

Since both CaO and $CaSO_4$ tend to hydrate upon exposure to moisture in the air, it was found preferable to deliberately hydrate the samples completely prior to analysis. Extensive analysis of the samples, and experiments to determine the rate of hydration of $CaSO_4$, indicated that hydration resulted primarily in the formation of $CaSO_4 \cdot 1/2H_2O$ rather than the dihydrate. The hydration procedure used was as follows:

(1) Samples, as received in vials from the reactor, were uncapped and placed in an oven at 230 F and exposed to steam at 1 atmosphere for 2 hours. This time period was longer than needed for hydration of samples of lime, but the presence of sulfate in a sample markedly decreases the hydration rate.(2)

(2) The steam source was removed and the oven was purged with nitrogen for a period of 1 hour in order to remove any excess water vapor from the system.

---

* It is important to consider the composition of the particular material used in this study since it has been found that other samples obtained from the same quarry not only may have different compositions but also may display different reaction characteristics. For example, other samples of Limestone 2061 received from the Sponsor have shown a tendency for violent fragmentation upon heating to temperatures in the neighborhood of 750 F, whereas the stone used in these studies did not tend to fracture. The tendency to fracture, of course, bears an important relationship to reactivity because of the potential dependence of reactivity on particle size.

(3) Vials were then removed from the oven and capped prior to analysis.

The composition of the resultant hydrated samples was considered to be $CaCO_3 + Ca(OH)_2 + CaSO_3 + CaSO_4 \cdot 1/2H_2O$ + unreactive material. Thermogravimetric analysis was used to determine the carbonate and hydroxide content. It was observed that, with samples containing appreciable quantities of sulfite, decomposition of the sulfite (at about the same temperature as decomposition of the carbonate) could cause inaccurate and nonreproducible results. However, if the thermogravimetric analysis was carried out in an oxygen atmosphere, this interference could be eliminated; oxidation of the sulfite proceeds at temperatures intermediate between those for decomposition of the hydroxide and the carbonate under the conditions used.

The total sulfur content was determined by colorimetry as described in detail in the August 30, 1968, Summary Report.[3] Analysis for sulfate was made by a similar procedure, except that the slurry of sample, ion-exchange resin, and solvent was purged with nitrogen during the digestion process and hydrogen peroxide was omitted from the solvent so that the sulfite was decomposed with evolution of SO_2. The sulfite content of the sample was then obtained by difference.

A computer program written in time-share FORTRAN for the GE Mark II time-share system for calculation of degree of calcium utilization, effective sulfur pickup, and degree of calcination is shown in Appendix B. The data used and the computational results are shown in Appendix A. The program calculates the degree of calcination by two slightly different routes, so that an internal check on the analytical data was possible. The first route places strong emphasis on the loss of water and carbon dioxide observed in the thermogravimetric analysis. The second route places more emphasis on the total analysis of the sample. Usually, the two numbers obtained were within 1 or 2 percent (absolute), and the average of these numbers is reported in Table A-1. On occasion, when these two numbers did not agree, either the analysis was repeated or a choice was made on the basis of apparent consistency with the body of data for a run. Since each component of the sample was subjected to analysis, a second check on the self-consistency of the data was made on the basis of a total accounting of the sample; the quantities of each component in a sample were calculated, and the sum was compared with the sample weight. Generally, it was found that 96 to 102 percent of the sample was accounted for by summing over the four or five separate analyses that were made. Occasional results showing greater than 5 percent deviation from this range were either rejected, or samples were reanalyzed.

EXPERIMENTAL WORK AND DISCUSSION

Reaction of Limestone with SO_2

The reaction of limestone with SO_2 was studied in the dispersed-phase reactor under a variety of conditions to determine the effect of temperature, SO_2 concentration, oxygen concentration, and precalcination of the stone on the overall reaction process. For these studies, -140 + 200-mesh Limestone 2061 was used in all cases, and SO_2 and O_2 levels were 0.3 and 3 percent, respectively, unless otherwise indicated.

Several qualitative observations of the results of the study of the limestone-SO_2 reaction are noteworthy at this point. The reaction apparently begins immediately upon injection of stone into the reactor; there is no lag time such as that required for heat-up and initiation of calcination as shown in a later section of this report. Furthermore, the loss of CO_2 proceeds to a greater extent in the presence of SO_2 as shown in Figure 6. This implies that the initial reaction with SO_2 involves a direct displacement of the type

$$CaCO_3 + SO_2 \rightarrow CaSO_3 + CO_2 ,$$

and that the sulfurization reaction aids in the calcination of the stone rather than inhibiting the calcination through formation of a barrier to effusion of the CO_2. The results of Van Heek and Juntgen[4] also indicate this displacement type of reaction.

It should also be noted that all of the curves of sulfur pickup versus time, as shown in Figure 7, are concave downwards. This is important, for it implies that the rate of mass transfer to the particles is sufficiently large that it does not limit the reaction rate. That is, physicochemical processes occurring within the particles appear to be limiting the overall reactivity of the stone in these reactor experiments.

Several different means for correlating the SO_2 reaction data were attempted, but no single approach was equally applicable to all sets of data. For example, log-log plots of sulfur pickup versus time indicated that some of the sets of data could be adequately represented by an equation of the type

$$S = kt^{1/2},$$

where S is the sulfur pickup in mg SO_3/g calcine, and t is time in seconds. However, with other data sets, a more complex behavior was indicated, and a polynomial of the form

$$S = at - bt^2$$

could be used within the limits of accuracy of the observations. Values of a, b, and k obtained by least-squares fitting of these curve forms to the raw data are shown in Table 1. Also shown in Table 1 are standard deviations in S calculated for each of the curve forms for each run. It is obvious that no clear choice can be made between these two types of curves on the basis of how well they fit the data.

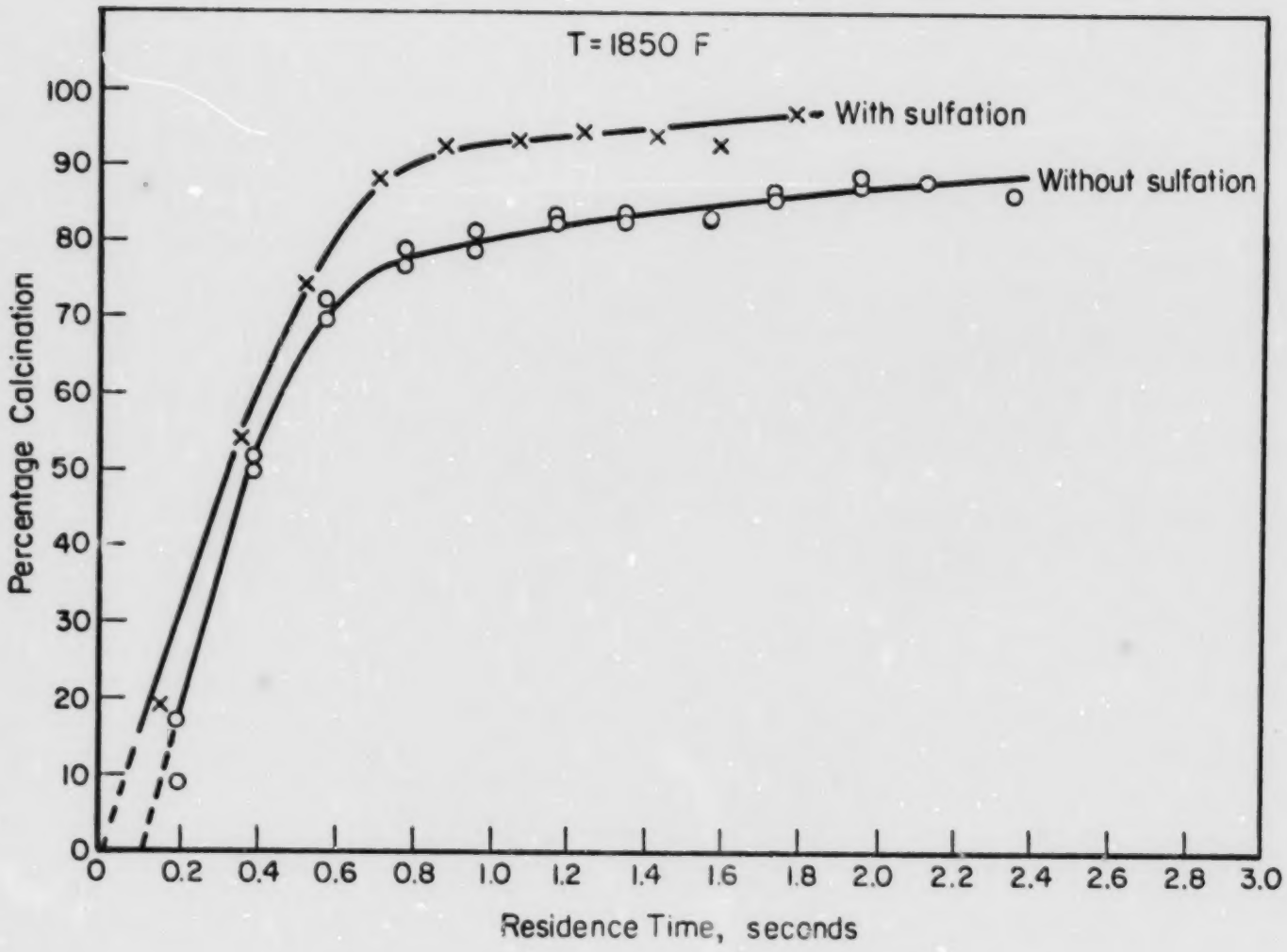

FIGURE 6. EFFECT OF SO_2 ON CALCINATION

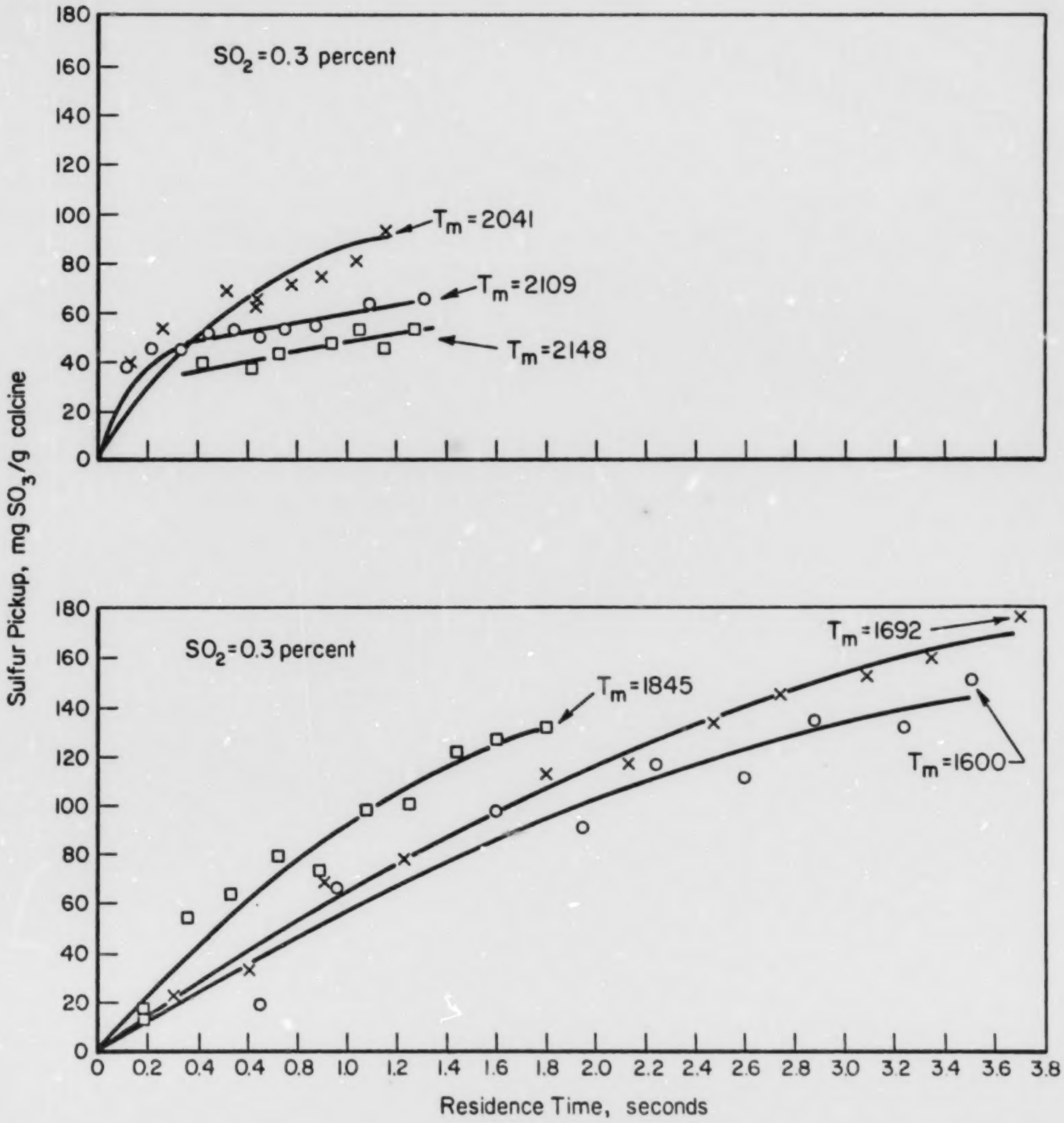

FIGURE 7. EFFECT OF TEMPERATURE ON SO_2 REACTION

TABLE 1. DATA CORRELATION

Run	T_m, F	$S = kt^{1/2}$ k	$S = kt^{1/2}$ Std Dev*	$S = at - bt^2$ a	$S = at - bt^2$ b	$S = at - bt^2$ Std Dev*	Comments
23	2041	87.4	17.4	154	71	11.7	Normal run with raw stone at 0.3 percent SO_2, 3 percent O_2
25	1600	74.3	9.3	62.7	6.19	12.0	
217	1845	93.8	8.1	115	23.6	6.86	
219	2109	59.8	10.2	132	68.5	9.93	
325	1692	84.8	9.9	71.4	6.84	5.39	
326	2148	49.7	8.1	105	54.3	8.65	
49	1717	70.8	7.5	74.6	10.9	13.6	Precalcined stone
410	1945	78.7	12.3	131	41.7	18.2	Precalcined stone
415	1711	54.0	7.6	49.5	5.74	5.9	O_2 = 0.4 percent
416AY	1717	89.8	13.4	94.4	13.7	3.28	O_2 = 6 percent
416AAYY	1692	27.3	3.7	33.2	5.99	4.44	SO_2 = 0.04 percent
417AY	1703	143.0	27.2	124	11.7	13.7	SO_2 = 0.95 percent
417AAYY	1690	122.3	14.9	113	12.3	3.86	SO_2 = 0.75 percent

* Standard deviation in S, mg SO_3/g calcine.

Effect of Temperature

Data for runs made at mean gas temperatures of 1600, 1692, 1845, 2041, 2109, and 2148 F are summarized in Figure 7. Figure 8 shows the alternative rate constants a and k from Table 1, plotted versus the mean gas temperature. Very little change with temperature is seen for k. The constant for the initial rate, a, however, is quite strongly dependent on temperature. It is apparent from Figure 8 that more or less regular increases in reaction rate and overall reactivity occur for increasing temperature up to about 1900 to 2000 F,* but above this point the reactivity drops off sharly.

* A similar maximum in reactivity has been observed in pilot-scale studies by workers at Babcock & Wilcox Co. as reported at the International Dry Limestone Injection Process Symposium at Gilbertsville, Kentucky, June 22-26, 1970.

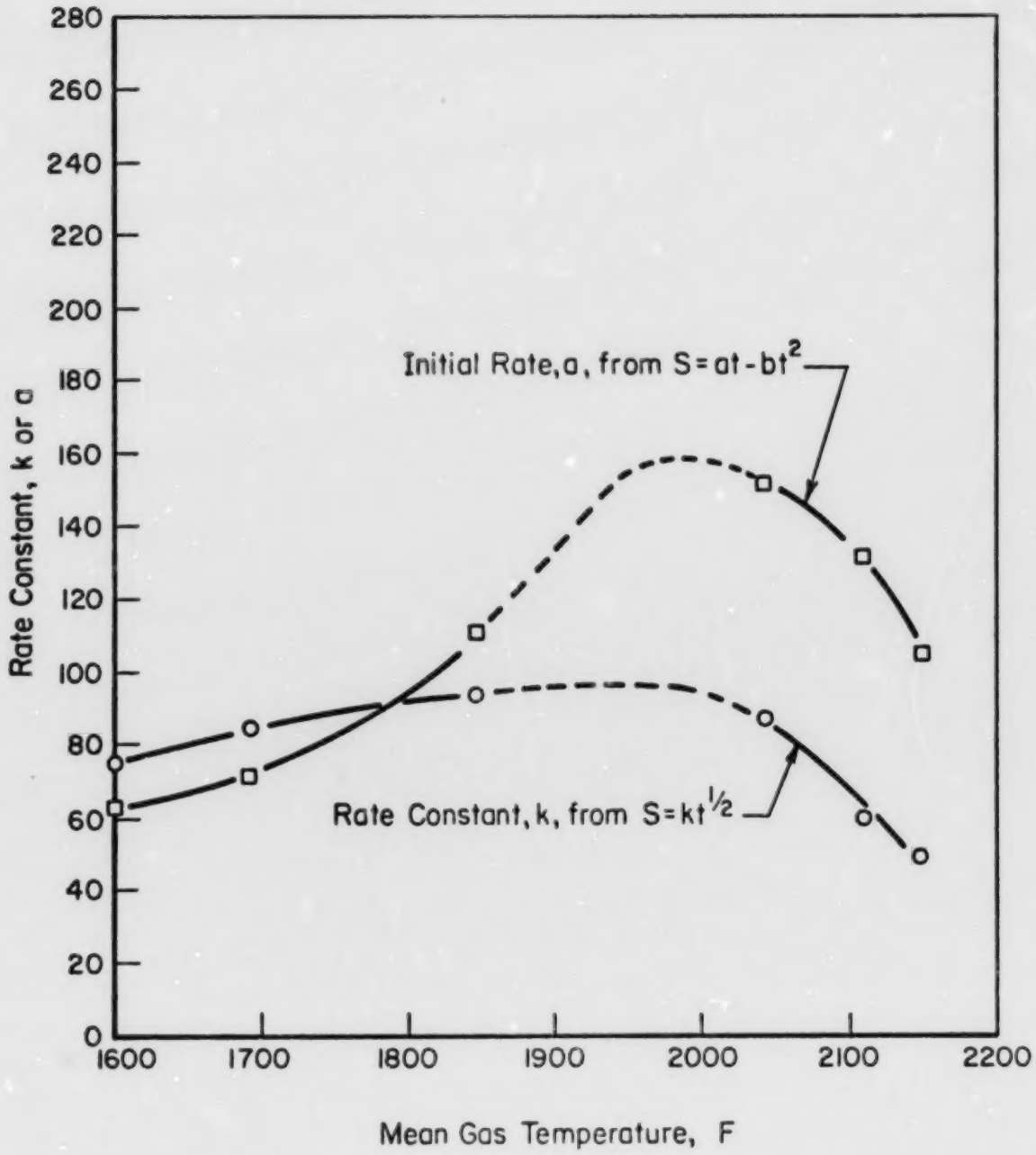

FIGURE 8. EFFECT OF TEMPERATURE ON REACTION RATE

An Arrhenius plot of the initial reaction rates for the three lower temperatures, 1600, 1692, and 1845 F, at various sulfate loadings, indicates an apparent activation energy of 10 to 12 kcal/mole. These values are in agreement with previous estimates[1] of the activation energy for Limestone 2061. It should be pointed out, however, that the apparent activation energy is critically dependent upon the choice of curve or mathematical model used to represent the data. If, for example, the equation $S = kt^{1/2}$ is used to represent the data, the apparent activation energy is about half that indicated above, hence the need for adequate modeling of the reaction process, especially at temperatures above 2000 F where reactivity apparently declines with increasing temperature.

Figure 9 shows a comparison of the average time-temperature profile of the Shawnee boiler (obtained from D. Clay of NAPCA) with that of the dispersed-phase reactor for several mean gas temperatures. Curves for the reactor are displaced along the time axis for convenience in comparison. It is seen that for operation of the reactor at a mean gas temperature of 2148 F, the time-temperature profile of the reactor closely parallels that of the injection section of the boiler. Assuming that the reactor data can be directly correlated with the boiler performance,* it would appear that no more than a few percent reaction would take place in this section, and little would be gained by use of the highest-temperature injection ports in the boiler. On the contrary, injection at the highest temperatures increases the risk of dead-burning of the lime and exceeding the thermal stability of $CaSO_4$, and hence decreases the chance for good overall reaction efficiency.

The reactor run at 2041 F is seen to approximate reasonably well the boiler profile between the lowest-temperature injection port and the secondary superheater section. Although this temperature is slightly above the point of maximum reactivity in the reactor, indications are that use of the lowest-temperature injection port on the boiler at about 2100 F may be best. Little direct comparison can be made between the reactor and the boiler at lower temperatures; Clay's data for the Shawnee boiler indicate that temperatures in the secondary superheater and reheater sections of the boiler appear to drop off much more quickly than those in the reactor. Further modeling of the reaction system and additional experimental work are needed to adequately correlate data from the reactor with the performance of the boiler at temperatures below 2000 F.

Modeling of the sulfurization reaction and means of correlation of reactor data with boiler performance are discussed further below.

---

* The validity of this assumption is very critical. However, at this point, not enough information is available from full-scale boiler tests of the process to enable judgment of the applicability of reactor results to prediction of boiler performance.

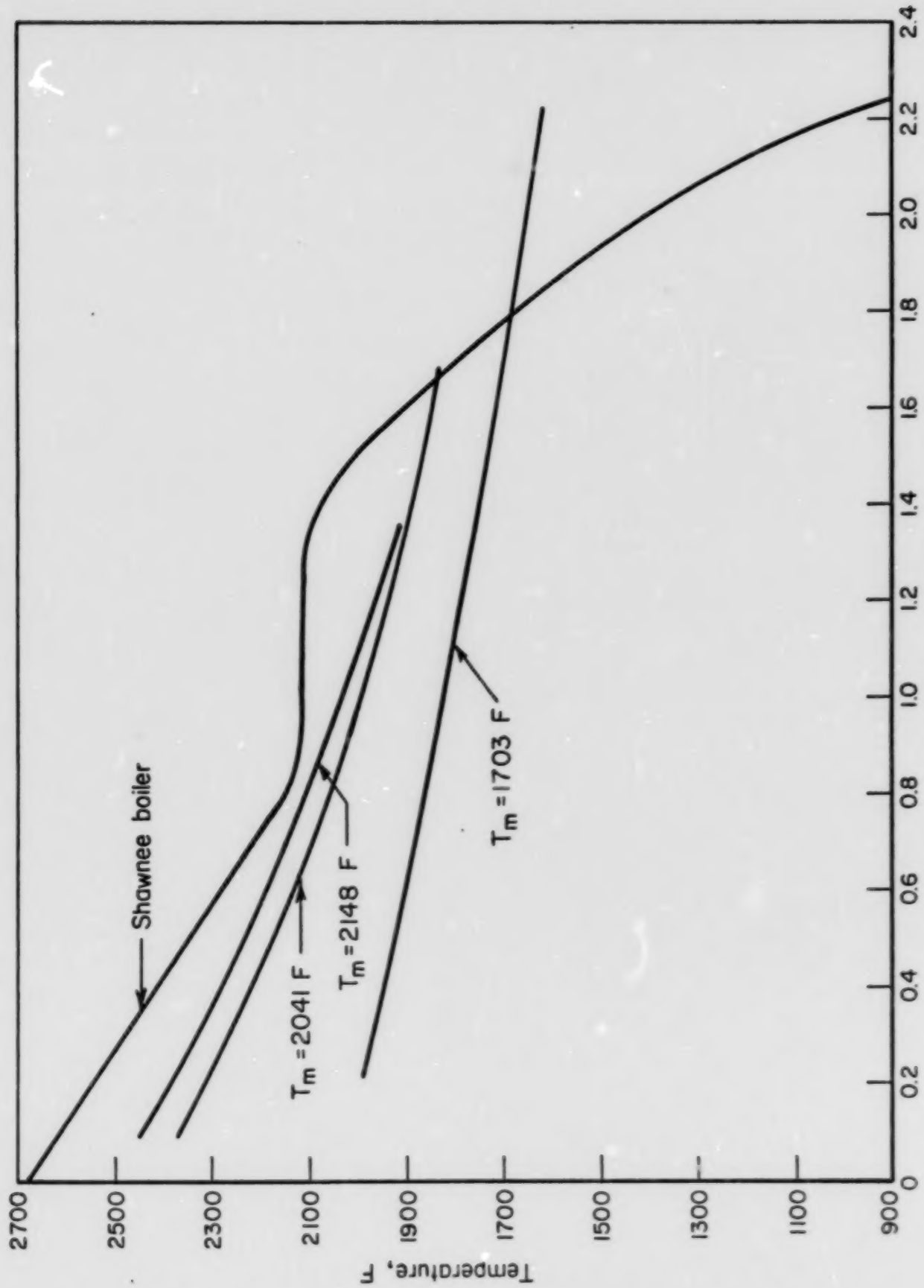

FIGURE 9. COMPARISON OF REACTOR WITH SHAWNEE BOILER--
TIME-TEMPERATURE PROFILE

Alternative Correlation Procedures

As mentioned, several different approaches can be taken to correlation of the current sulfurization data. As indicated above, a simple polynomial or power-law type of expression might be fitted to the data, and the comparison could be made between the coefficients of the equations obtained for various modes of operation of the reactor. However, this approach may not be useful in extrapolating from reactor results to boiler performance, especially under conditions where the time-temperature profile of the boiler is markedly different from that in the reactor. If the real temperature dependence of the process is appreciable, large errors are likely to result from direct extrapolation. It is therefore desirable to develop other means for data correlation which take account of the actual time-temperature profile of the reactor. One such procedure is given below.

At constant SO_2 and O_2 concentration, and for a given particle size, the only measured variables of the reacting system were sulfur pickup, time, and temperature. Since Borgwardt[5] has found that the reaction is self-inhibiting, an empirical equation of the following type might be used to represent the rate of reaction at any instant:

$$\frac{dS}{dt} = A\, S^{-n}\, e^{-E/RT^*} , \qquad (1)$$

where S is the sulfur pickup in mg SO_3/g, A is analogous to the Arrhenius frequency factor, E is the apparent activation energy, and T is the particle temperature. As seen later in the discussion of calcination, the particle temperature is generally lower than the gas temperature at reaction times of interest, but is dependent to some extent upon the gas temperature. For the current purposes of gaining a first approximation, the particle temperature in Equation (1) has been replaced by the gas temperature, recognizing that this is only an approximation and perhaps not a very good one at residence times of less than 0.5 second.

Equation (1) can be integrated numerically if the gas temperature is expressed as a function of time. As indicated earlier, the gradient in the reactor is nearly constant, and a linear function can be used. In practice, it is convenient to express both the time and temperature in terms of distance, ℓ, along the reactor. The temperature can be expressed as

$$T = T_m + a(6-\ell),$$

where T_m is the centerline temperature at the middle reactor port (ℓ = 6 ft), and a is determined for each run from the measured temperature gradient. It was also found by examination of the data that the residence time is proportional to distance traveled, with fairly good accuracy, so that

$$dt = C\,d\ell ,$$

where C is a constant.

---

* It should be noted that when $n = \frac{1}{2}$ the form of this equation is equivalent to the simple power law, $S = kt^{1/2}$, except for inclusion of the specific temperature dependence of the rate constant.

The function to be used to correlate the data thus becomes

$$\frac{dS}{d\ell} = ACS^{-n} \exp -E/R[T_m + a(6-\ell)] \quad . \qquad (2)$$

Rearranging Equation (2) and integrating between S=0 at $\ell=\ell_1$ and S=S at $\ell=\ell_2$,

$$\frac{S^{n+1}}{n+1} = AC \int_{\ell_1}^{\ell_2} \exp - [E/R(T_m + a(6-\ell] \, d\ell \quad . \qquad (3)$$

The form of Equation (3) is potentially useful in that it allows both evaluation of the reactor data and prediction of the boiler performance on the basis of the reactor evaluation. The main requirement for this is that it be shown that the equation does indeed adequately represent the reaction. Of course, the dependence of the frequency factor, A, on SO_2 concentration, O_2 concentration, and particle size must also be demonstrated.

A computer program, shown in Appendix C, was developed for evaluation of the data with respect to Equation (3). This program was written in time-share FORTRAN for use with the GE Mark II time-share system, and employs a GE proprietary subroutine (LSQMM). The basic operation of the program involves input of data for all runs along with a trial set of E's. The computer then makes a least-squares fit of Equation (3) in log-log form to determine the best values of n and A for each value of E and computes the standard deviation of S. The standard deviation may then be used as a criterion for choice of a new set of E's, and the process is repeated until a minimum standard deviation is found for a particular set of n,A, and E. These "best" values of n,A, and E may then be used to calculate values of S as a function of time. Preliminary use of this program has shown that the evaluation of n,A, and E is quite sensitive to the apparent quality of the input data; for data that appear to have considerable scatter, no reasonable fit can be obtained. However, in the case of the data for the sulfurization reaction at 1692 F, where there is little scatter, the standard deviation is minimized quite sharply at E = 22,000 cal, n = 0.25, and $A = 1.5 \times 10^7$. Use of these values allows reasonably good prediction of the reactivity at 1600 and 1845 F.

Although Equation (3) seems to adequately represent the low-temperature data, obviously it cannot predict performance at temperatures greater than about 1950 F where reaction rates start to fall off with increasing temperature. Further development, taking account of what is obviously a competing or limiting reaction, is needed in this temperature region. One obvious limiting factor for the reaction at the higher temperatures involves the dissociation of $CaSO_4$. With this in mind, the system might be approximately represented in terms of the reaction.

$$CaO + SO_2 + 1/2O_2 \underset{2}{\overset{1}{\rightleftharpoons}} CaSO_4 \quad .$$

It is seen from this equation that as the temperature is increased to near the equilibrium condition, or if the SO_2 pressure is decreased by sorption, further reaction will be severely limited. Another factor that should be considered at these higher temperatures is sintering of the lime.

Effect of SO_2 Concentration

Several exploratory runs were made to gain some overview of the dependence of reaction rate on SO_2 concentration. Data for runs made with SO_2 concentrations of 0.05, 0.3, 0.75, and 0.95 percent are summarized in Figure 10. For convenience at this point, the data for these runs were represented in terms of a second-order polynomial of the form

$$S = at - bt^2,$$

so that the coefficient "a" represents the initial slope, or initial reaction rate, which can be used to correlate reactivities at the various SO_2 levels. It must be emphasized that this representation is not necessarily correct nor even the best representation. However, it does provide a means for correlating the data at this point.

Furthermore, since only four different concentrations were considered in these exploratory runs, there may be considerable error in any tentative conclusions based on the results. This possibility is strengthened by the fact that for the one run at an SO_2 concentration of 0.04 volume percent, the extent of reaction did not go beyond the equivalent of about 3 percent utilization of the lime. Hence, only three of the runs can be compared for SO_2-concentration dependence over a range of sulfate loadings. To make this comparison the apparent rates of reaction were determined at a series of sulfate loadings, S (mg SO_3/g), and $\log(\frac{dS}{dt})$ was plotted versus $\log C_{SO_2}$ for each value of S. The apparent order of reaction with respect to concentration was determined from the slope of the log-log plot. Figure 11 shows plots obtained at selected loadings; Table 2 lists in more detail the apparent reaction orders obtained at various loadings. These data show that the apparent reaction order changes in a regular fashion from about 0.5 to S = 0 to 1 to even greater than 1 at higher values of S. Obviously, some further work needs to be done in this area. However, the current data seem to indicate a changing mechanism and changing importance of SO_2 concentration as the reaction progresses. If this tentative conclusion is correct, then in a boiler, where the SO_2 concentration drops off as the reaction proceeds, the rate of reaction will decline more rapidly with time than is shown in the reactor results.

Effect of Oxygen Concentration

It was noted in previous work[1] that the initial chemical step in the sulfurization of limestone may involve the formation of calcium sulfite, and that subsequent oxidation or disproportionation of the sulfite to sulfate is necessary for retention of appreciable quantities of sulfur by the limestone. The rate of

the oxidation reaction would be expected to be dependent on the concentration of oxygen in the flue gas, but the rate of the disproportionation reaction probably is independent of oxygen content. In the current work a limited number of runs were performed to obtain a qualitative picture of the dependence of the rate of the SO_2 reaction on oxygen concentration. Data for these runs at oxygen levels of 0.4, 3.0, and 6.0 percent are summarized in Figure 12. Rates of reaction were determined at various sulfate loadings as above, and a log-log plot of rate versus oxygen content is shown in Figure 13. Although the data are limited and any conclusions must be considered as tentative, the data suggest that at low concentrations and low sulfate loadings, the rate may level off and become relatively independent of oxygen concentration, whereas at higher O_2 levels and higher sulfate loadings, the rate is more strongly dependent on the oxygen concentration. These observations are consistent with the notion of two chemical routes to sulfate formation, i.e., disproportionation and direct oxidation. However, as with the SO_2-concentration data, the dependence is a function of sulfate loading, indicating that factors other than the chemistry of the process are influencing the observed rates.

The data do indicate that more rapid reaction and possibly more efficient capture of SO_2 might be obtained in a boiler if the excess air were increased somewhat. It should be noted that the decomposition of $CaSO_4$ will be shifted to higher temperatures if the O_2 content is raised, so that higher injection temperatures may be possible, if overburning of the lime is not a serious factor.

TABLE 2. APPARENT ORDER OF REACTION WITH RESPECT TO SO_2

Sulfate Loading, mg SO_3/g calcine	Apparent Order
0	0.49
10	0.50
20	0.51
30	0.52
40	0.53
50	0.55
60	0.56
70	0.58
80	0.60
90	0.63
100	0.66
110	0.69
120	0.73
130	0.78
140	0.84
150	0.92
160	1.04
170	1.23
180	1.63

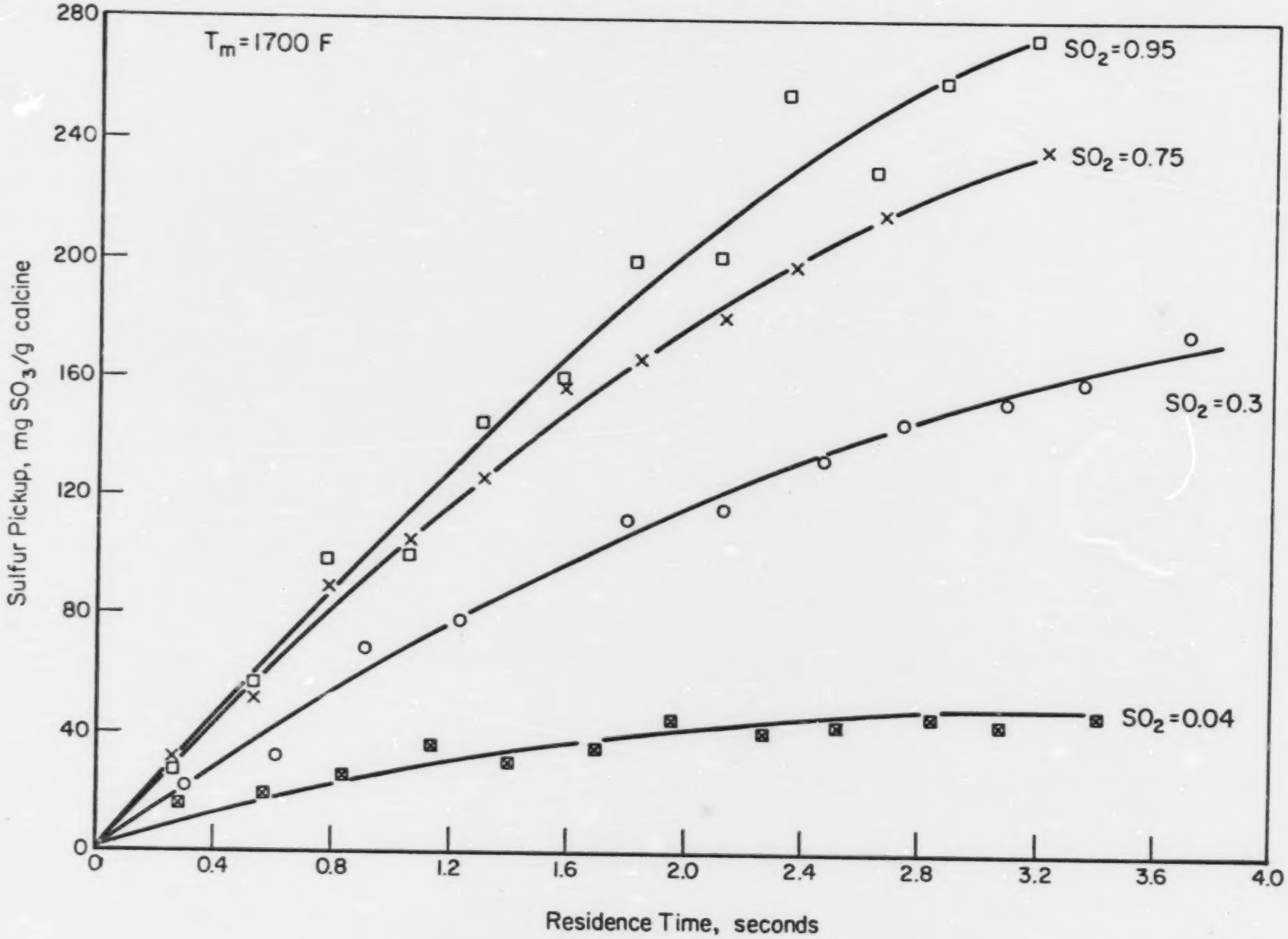

FIGURE 10. EFFECT OF SO_2 CONCENTRATION ON REACTIVITY

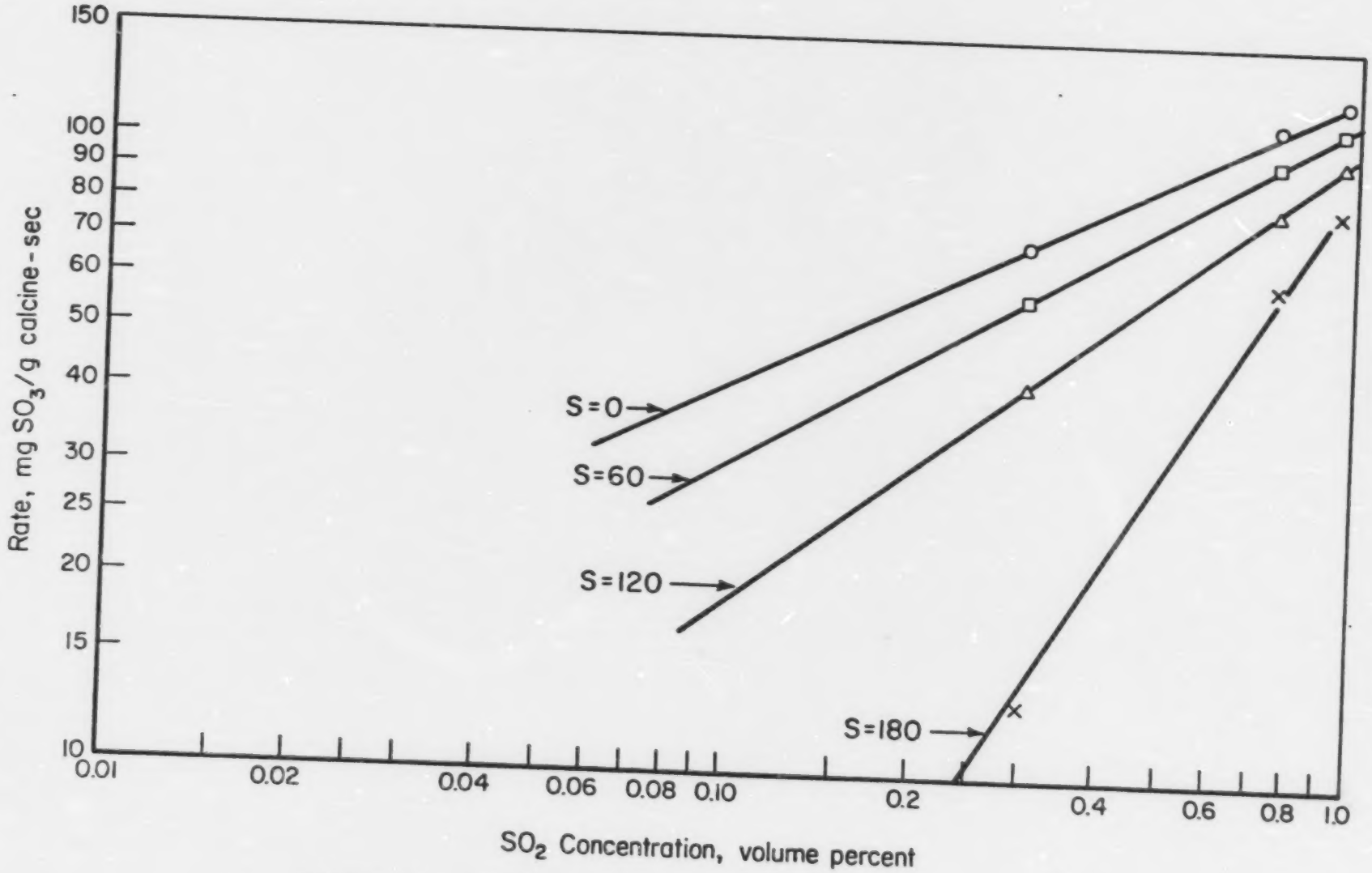

FIGURE 11. DEPENDENCE OF SULFATION RATE ON SO_2 CONCENTRATION AT VARIOUS SULFATE LOADINGS

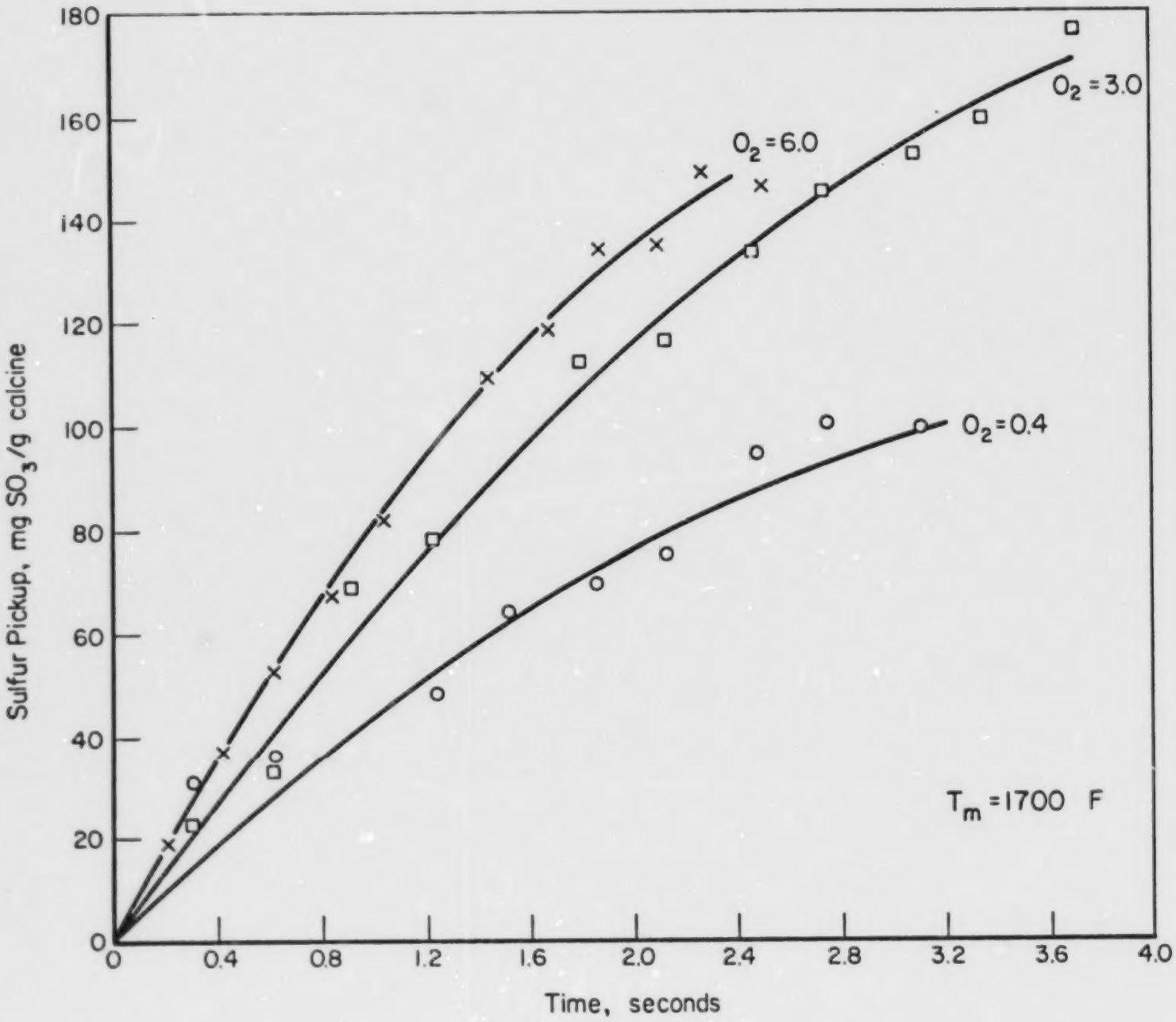

FIGURE 12. EFFECT OF O_2 CONCENTRATION ON REACTIVITY

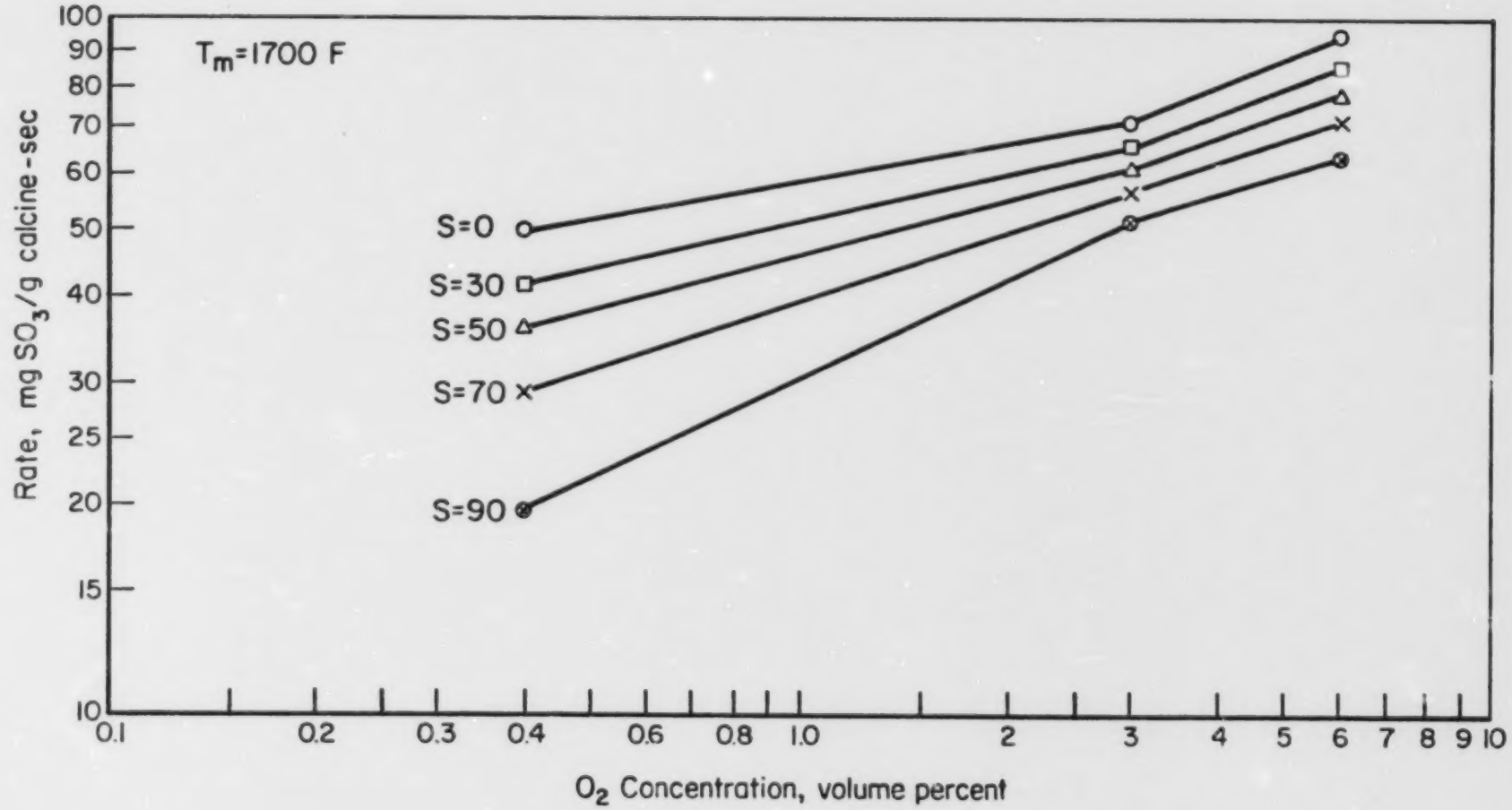

FIGURE 13. DEPENDENCE OF REACTION RATE ON O_2 CONCENTRATION AT VARIOUS SULFATE LOADINGS

Effect of Precalcination of Stone

In previous work[1] it was found that precalcination of limestone resulted in reduced overall reactivity toward SO_2. However, in all known previous work the burnt lime used has been obtained by calcination of stone for much longer periods of time (minutes to hours) than are available in the reactor or a boiler. In view of the known tendency for lime to sinter and eventually dead-burn, it was felt that the burnt limes used in this previous work might not be representative of burnt lime formed in a boiler by injection of raw stone. In the current work, runs were made with stone calcined for short periods of time to simulate the process as it occurs in the reactor or in a boiler. To do this, limestone was blown through a coil of Vycor tubing mounted within a tube furnace, and was then fed directly into the reactor through an uncooled stainless steel probe.

A schematic drawing of this calciner-probe arrangement is shown in Figure 14. The temperature in the calciner was approximately 1870 F, and the residence time was approximately 0.3 second. Samples of the calcined material were analyzed by thermogravimetric analysis and found to be about 65 percent calcined. Runs to determine the SO_2 reactivity of this material were made in the reactor at mean gas temperatures of 1717 and 1945 F. Results of these runs are summarized in Figure 15. Comparison of the results with those for raw stone indicates that the precalcined stone may react more readily in the first couple of tenths of a second of exposure in the reactor, but the rate very quickly decreases and the overall activity of the precalcined material is less than that for the raw stone.

Importance of Sulfite Formation

In previous work[1], it was found that appreciable amounts of calcium sulfite were formed during the early stages of reaction of SO_2 with limestone, and a correlation was suggested between the degree of calcination of the stone and the fraction of sulfur present as the sulfite. Although the meaning of this correlation is not fully understood, it is believed to be related to the fact that the temperature of the particle remains relatively low during the calcination process because of the thermal requirement for calcination. The theoretical model of the calcination process, discussed below, indicates that temperatures within the lime shell are generally higher than the decomposition point of the sulfite except during the initial stages of the reaction. It was found experimentally that the sulfite content does go through a maximum during these initial reaction stages.

Figure 16 shows a plot of the fraction of sulfite present as a function of percentage calcination for all of the runs made during the current work. Although there is considerable scatter in the data, the fraction of sulfur present as sulfite is definitely higher at a low extent of calcination and some correlation seems evident. Inclusion of data for runs with variable O_2, SO_2, and precalcined stone does not affect the scatter in this correlation. It is felt that use of this correlation may help significantly in development of a model for the reaction process and description of the details of the reaction.

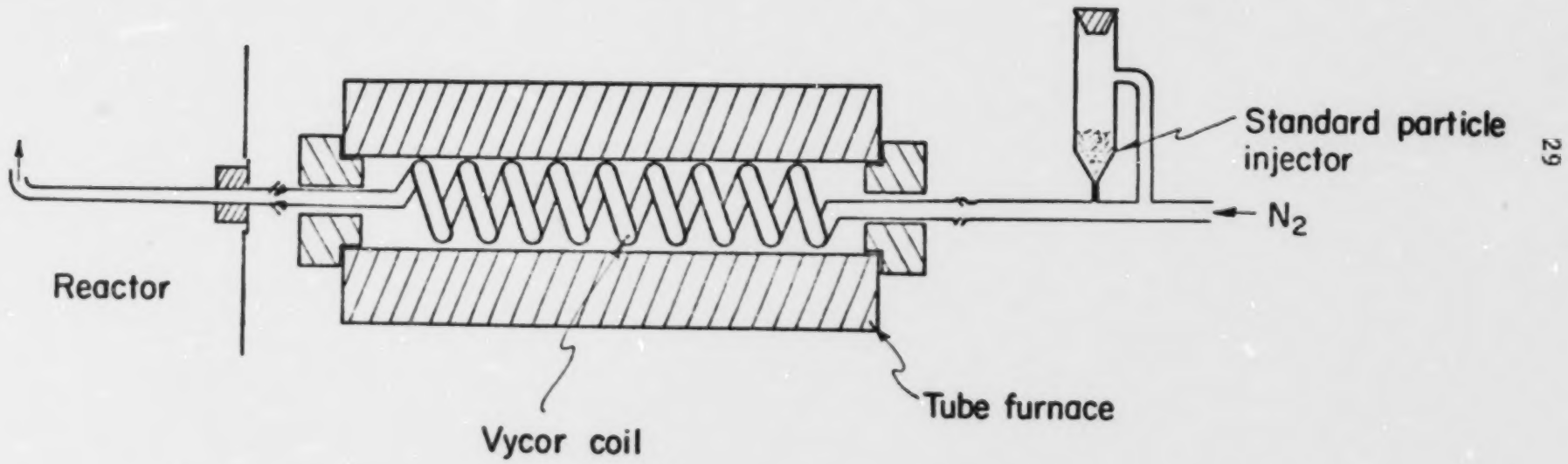

FIGURE 14. CALCINER -- INJECTOR

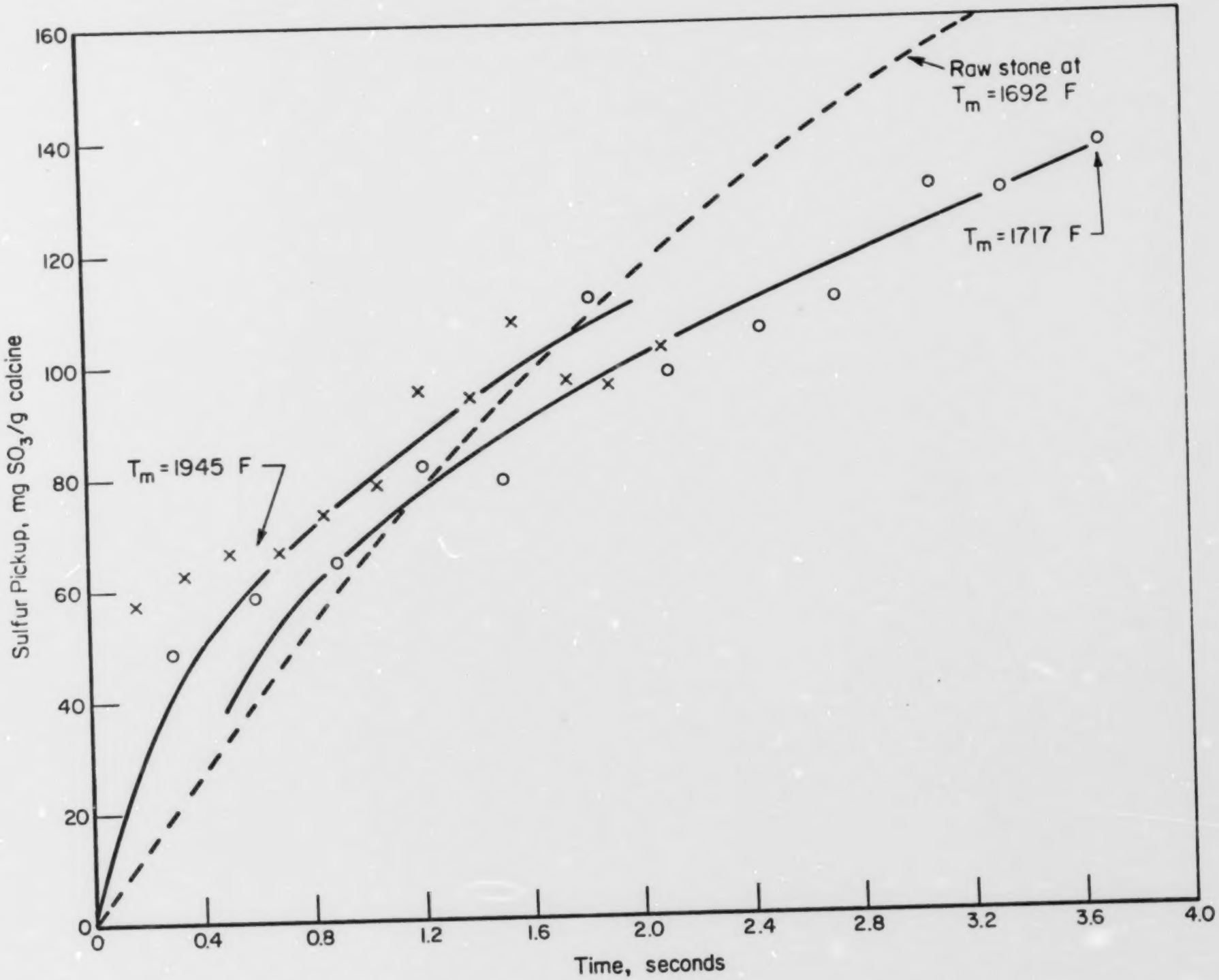

FIGURE 15. RUNS MADE WITH PRECALCINED STONE

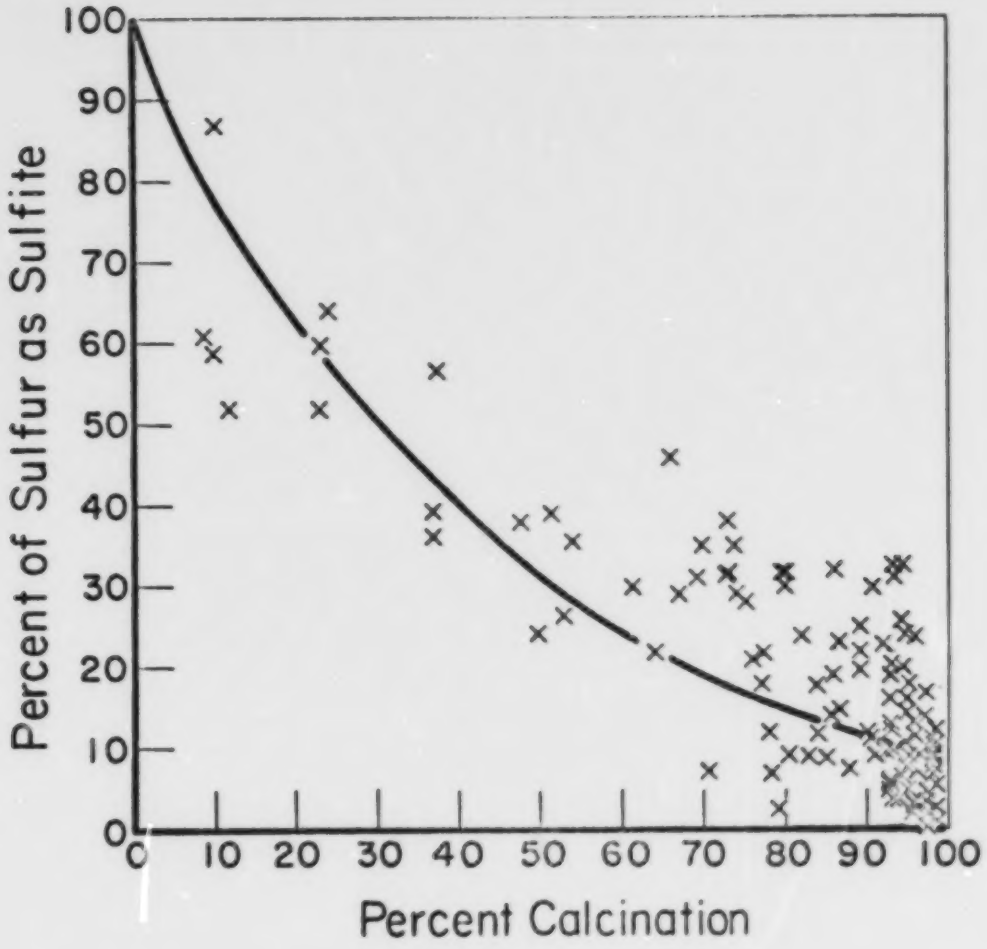

FIGURE 16. RELATION OF SULFITE CONTENT TO DEGREE OF CALCINATION

Calcination of Limestone

Basis of Representation

The rate of calcination of limestone is highly important in the overall process of sorption of SO_2 from flue gas by the stone. This is true whether the calcination and SO_2-sorption processes occur independently or in concert. Modeling of the dry-limestone-injection process must therefore be based on a well-developed representation of the calcination process.

The rate of calcination of limestone has been considered by many investigators[6-12], but, in the main, their representations have been relative to calcination of large (1 to 10 cm) pieces of stone under nearly isothermal conditions involving reaction times of minutes to hours. This process is distinctly different from the calcination of 10 to 100-micron particles of limestone within times of less than a second under highly nonisothermal conditions, as in the case for limestone injected into a boiler. Hills[12] and others[10,11] have shown that calcination of limestone under the former conditions can be adequately represented by a steady-state model of heat and mass transfer within the porous lime. The steady-state representation cannot, however, be applied to the real situation in boiler furnaces; the heat-transfer coefficient is much larger for the smaller particles, and both temperature and pressure change very rapidly. Further, the temperature gradient is not adequately represented by an inverse function of the square of the radius as it is for steady-state conditions.[13] Representation of the calcination process relative to injection of limestone into a boiler requires a non-steady-state model. Such a model is developed below (see Figure 17).

Model of Calcination Process

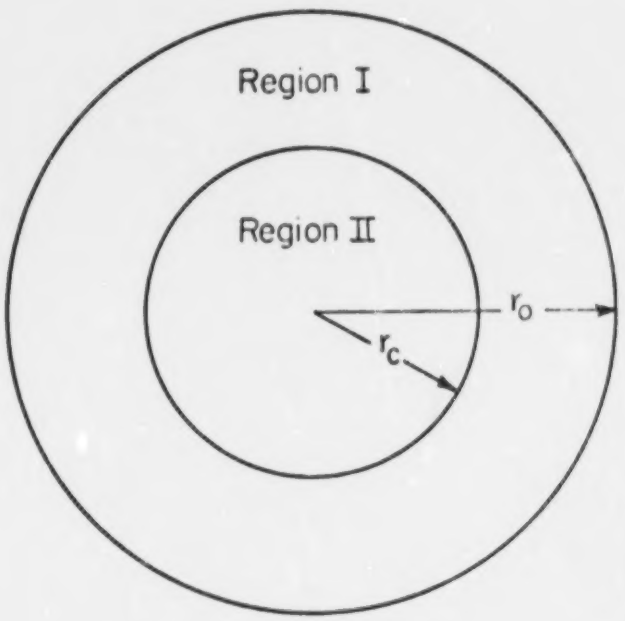

I. Lime shell,
$T = T(r,t)$
$P = P(r,t)$

II. Carbonate Core,
$T = T_c(P,t)$

FIGURE 17. PARTLY CALCINED SPHERICAL LIMESTONE PARTICLE

Consider a spherical limestone particle of radius r_o at an initial temperature T_o, injected into a flue-gas stream at temperature T_g. For simplification of the problem, it is assumed that the walls of the reaction chamber are at the same temperature as the flue gas, and that the initial process of heatup of the particle from T_o to T_c (the temperature at which the equilibrium partial pressure of CO_2 is equal to the pressure of CO_2 in the flue gas) can be treated independently from the calcination process. The latter assumption is equivalent to saying that the thermal diffusivity of calcium carbonate is sufficiently large that the particle remains essentially isothermal during the initial heatup. The validity of this assumption is borne out by results shown later. It is also assumed in this model that the chemical reaction rate does not limit the process.

The time required to heat a spherical limestone particle from injection temperature, T_o, to decomposition temperature, T_c, may be calculated as follows:

$$\dot{q} = 4\pi r_o^2 h(T_g - T) \quad , \tag{1}$$

where h is the sum of the heat-transfer coefficients for radiation and convection, respectively, and can be evaluated[11] from

$$h = \epsilon\sigma (T_g^4 - T^4)/(T_g - T) + \frac{k_g}{2r_o}\left[2 + 0.37\ (N_{Re})^{0.6}\right] \quad , \tag{2}$$

where ϵ is the emissivity, assumed to be the same for the particle and the Alundum reactor wall, σ is the Stefan-Boltzmann constant, k_g is the mean thermal conductivity of the flue gas, and N_{Re} is the Reynolds number for flow of gas around the particle. For a 90-micron particle in the reactor, N_{Re} is small and the term in brackets in Equation (2) is very close to 2. For an isothermal, spherical particle, the rate of absorption of heat within the particle is

$$q^{\cdot} = \frac{4\pi r_o^3}{3} S_{II}\rho_{II}\left(\frac{dT}{dt}\right) \quad , \tag{3}$$

where S_{II} and ρ_{II} are the specific heat and density of the limestone. Hence, from Equations (1) and (3), the rate of change of the temperature of the particle is

$$\left(\frac{dT}{dt}\right) = \frac{3h}{S_{II}\rho_{II}r_o}(T_g - T) \quad . \tag{4}$$

Equation (4) can be rearranged and integrated numerically [h = f(T)] to find the time required for heat-up of the particle from $T = T_o$ to $T = T_c$. As will be seen from examination of the experimental data, heat-up times in the reactor are generally of the order of a few tens of milliseconds, in quite good agreement with calculated values obtained by Equation (4). It should be noted at this point that the contribution of radiation to the overall heat transfer is relatively low for small particles at temperatures below about 2000 F, and, therefore, the assumption that the wall temperature is equal to the gas temperature is not important to most runs being made in the dispersed-phase reactor.

Once the temperature of the sphere reaches T_c, calcination will commence and proceed radially inward. The value of T_c is determined by the pressure of CO_2 in the gas phase at the calcination boundary. Since it is assumed that the chemical reaction rate does not limit the process, this pressure is given by

$$P_c = \exp\left(-\Delta F^o_{T_c} / RT_c\right) \quad , \tag{5}$$

where $\Delta F^o_{T_c}$ is the standard free energy of dissociation of calcium carbonate at the calcination temperature, T_c, and R is the gas constant.

From this point on, the calcination process is considered in terms of a non-steady-state model.* Within Region I, the continuity equation for heat flow is

$$k \nabla^2 T = S_I \rho_I \left(\frac{\partial T}{\partial t}\right) + v_g S_g \rho_g \left(\frac{\partial T}{\partial t}\right) \quad , \tag{6}$$

where k, S_I, and ρ_I are the thermal conductivity, specific heat, and density of the lime; S_g and ρ_g are the specific heat and density of the CO_2 within the pores; and v_g is the velocity of the CO_2 flowing through the porous structure. The second term on the right side of Equation (6) thus accounts for heat withdrawn from the particle by the outward gas flow. The gas velocity at any point in the lime shell can be obtained from

$$v_g = \frac{\varepsilon D}{\rho_g}\left(\frac{\partial \rho_g}{\partial r}\right) \quad , \tag{7}$$

where ε is the porosity and D is the diffusion coefficient given by Knudsen's equation for molecular and viscous flow.(12)

$$D = \frac{2a}{3}\sqrt{\frac{8RT}{M\pi}} + \frac{a^2}{8\eta}P \quad . \tag{8}$$

Here, a is the pore radius, M is the molecular weight of the CO_2, and η is the viscosity of the CO_2.

Within Region II, it is assumed that heat transfer is essentially instantaneous, as was assumed in consideration of the initial heat-up. Since most of the heat arriving at the decomposition boundary at r_c will be used in the calcination process, the rate of temperature rise in Region II will be relatively low and this approximation should be quite good.

---

* Mass flow is treated in steady-state terms, whereas heat flow is considered as a non-steady-state process. Justification for this type of approach in general has been given by C. Y. Wen at the International Dry Limestone Process Symposium, Gilbertsville, Kentucky, June 22-26, 1970.

Boundary conditions for the process are:

(1) For heat balance at the calcination front,

$$k\left(\frac{\partial T}{\partial r}\right)_{r=r_c} - \frac{r_c}{3} S_{II}\rho_{II}\left(\frac{\partial T_c}{\partial t}\right) = - L\rho_{II}\left(\frac{\partial r_c}{\partial t}\right) , \qquad (9)$$

where L is the heat of calcination.

(2) At the particle surface,

$$P_{r_o} = P_{CO_2} , \qquad (10)$$

For heat balance at the particle surface,

$$-k\left(\frac{\partial T}{\partial r}\right)_{r=r_o} = h(T_g - T_{r=r_o}) + (S_g\rho_g v_g)(T_g - T_{r=r_o}) . \qquad (11)$$

Numerical methods must be used for solution of this problem, and a computer program, shown in Appendix D, has been developed for the purpose. The program was designed for use with the GE Mark II time-share system and is written in time-share FORTRAN. Results obtained thus far are in reasonably good agreement with experimental results, and further development of the model relative to calcination and reaction with SO_2 seems justified.

Effect of Porosity on Thermal Conductivity

The effect of porosity on the thermal conductivity of lime previously has been ignored in modeling the calcination process. This parameter may well be considered as a constant in modeling of the calcination process by conventional lime-burning procedures that give soft-burned limes of near theoretical porosity, 55.5 percent.(16) However, in considering the dry-limestone-injection process, porosity is expected to vary considerably, depending on the gas temperature at the injection point. Injection with the fuel, for example, has been shown to lead to considerable dead-burning of the lime.(17)

In principle, the thermal conductivity of a porous structure may vary from nearly that of the solid to nearly that of the gas within the pores, depending on the degree of porosity. Dul'nev has provided a model of thermal conductivity in such porous structures on the basis of a series-parallel representation of conduction paths in the porous structure.(18) Dul'nev views the porous solid as an interconnecting network of pores with a unit cell as given in Figure 18. Here, h/2 = thickness of the solid lattice member, ℓ = pore size, and L = h + ℓ = height of the unit cell. For this structure, and in consideration of the series-parallel paths of conduction within the cell, Dul'nev gives the conductivity of the structure as:

$$\lambda = \lambda_1 \left[\left(\frac{h}{L}\right)^2 + \nu\left(1 - \frac{h}{L}\right)^2 + \frac{2\nu h}{L}\left(1 - \frac{h}{L}\right) \Big/ \left(1 - \frac{h}{L}(1 - \nu)\right) \right] ,$$

where λ_1 is the conductivity of the solid phase, and λ_1 is the conductivity of the gas phase. To determine h/L from the porosity, ϵ,

$$\frac{h}{L} = \frac{h/\ell}{1 + h/\ell} ,$$

$$h/\ell = x/(0.5 - x) ,$$

and

$$4x^3 - 3x^2 + \frac{1 - \epsilon}{4} = 0 .$$

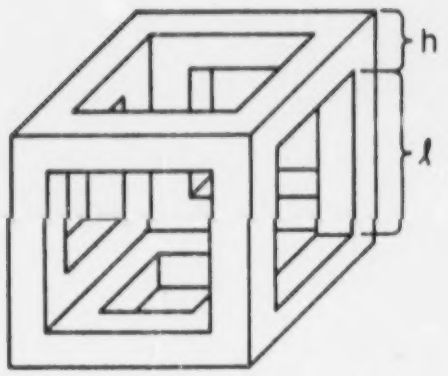

FIGURE 18. MODEL OF A POROUS SOLID

Figure 19 shows the calculated effects of porosity on the thermal conductivity of lime with CO_2 within the pores. It can be seen that the effective thermal conductivity of soft-burned lime (ϵ = 0.55) is only about one-fourth that of hard-burned lime. Thus, if dead-burning of the lime can occur quickly enough during the calcination process, it may have a significant effect on the rate of calcination. Of course reduction of porosity will also alter the mass-flow rate and tend to restrict the calcination process.

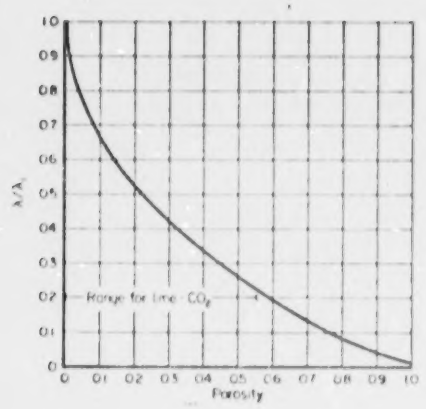

FIGURE 19. EFFECTIVE THERMAL CONDUCTIVITY OF CO_2-FILLED LIME

Experimental Studies

The calcination of Limestone 2061 was studied in the absence of SO_2 in the dispersed-phase reactor at mean gas temperatures of 1600, 1770, 1863, and 2068 F.

Figures 20 through 24 show the results of the calcination experiment at these temperatures. It can be seen by extrapolation to zero percent calcination that a measurable time of roughly 0.04 to 0.08 second is required for heat-up of the particles before calcination can commence, and that the extent of calcination does not go beyond 90 percent within the time available in the reactor.

Also shown in these figures are theoretical calcination curves obtained using the above model, assuming constant gas temperature, T_g, and a pore radius of 0.1 micron. In general, theoretical curves are parallel with the experimental curves and could be adjusted to match the experimental curves by adjustment of the pore radius to a lower value. Also, some allowance should be made for the fact that there are significant temperature gradients in the reactor.

The data show approximately the same rate of calcination for -140+200-mesh stone and -270+325-mesh stone at 1770 F (Figures 20 and 23). Comparison of the data indicates that the measured rate of calcination of -140+200-mesh stone at 1770 F is too high to be consistent with rates determined at other temperatures. Therefore, the data for -140+200 stone at 1770 F should be considered in error, and the question of size dependence remains unanswered. The theory suggests a very strong dependence of rate of calcination on particle size as implied by the curve in Figure 20, but this aspect remains to be checked in practice.

Effect of Gas Temperature. Choice of temperature of injection in the dry-limestone process is limited and dependent on boiler design, but it may be critical to overall performance. Figure 25 shows an Arrhenius plot of theoretical and experimental rates of calcination determined during this period. For the

purpose of plotting, rate was defined as the reciprocal of the time required for 50 percent calcination ($t_{1/2}$). Ignoring the 1770 F point, which appears to be in error as discussed previously, it may be seen that the calculated and experimental rates have the same temperature dependence, giving an "apparent activation energy" of about 18 kcal/mole and indicating the general validity of the model.

Effect of Pore Size. In the current model of the calcination process, the pore radius has been treated as a constant, adjustable parameter. Of course, in the real calcining particle, the pores are very small in the vicinity of the calcination front because some finite time must be allowed for development of pore structure from what is essentially a calcite pseudolattice. This implies that the pore structure should correctly be represented as having a continuously changing distribution of pore sizes. In principle, this type of representation could be made in terms of the rate of sintering of the limestone as a function of time and temperature. Such representation might be required in consideration of the process at high temperatures (e.g., 3000 F), where pore size and porosity may change very rapidly, but does not appear to be required for modeling relative to the calcination process in practical temperature ranges employed in the reactor or in a boiler. In the latter case, it appears adequate to use a single "average" pore size to represent pore structure.

Figure 26 shows the calculated calcination curves at 1770 F for three different pore sizes, 0.01, 0.1, and 1 micron, at constant porosity. It is obvious that the rate is less sensitive to pore-size changes for large pore radii than for small radii. Typical commercial soft-burned limes have average pore radii of the order of 0.1 micron, but in preparation of these limes, sufficient time is available for development of the pore structure by sintering. In the current calculations, a value of 0.1 micron was used, but comparison of the predicted and experimental rates indicates that a slightly smaller size may be more appropriate.

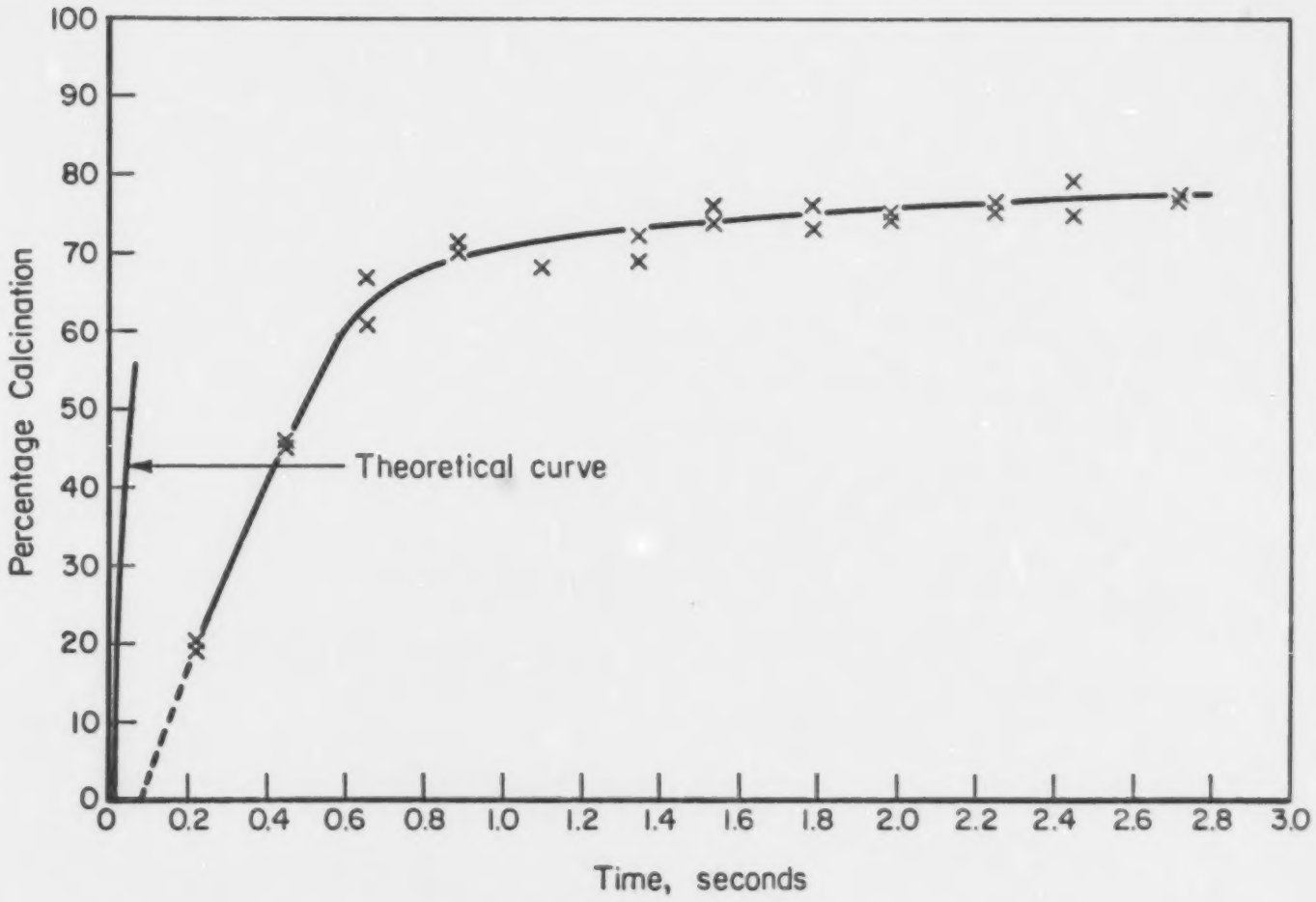

FIGURE 20. CALCINATION OF -270+325-MESH LIMESTONE AT 1770 F

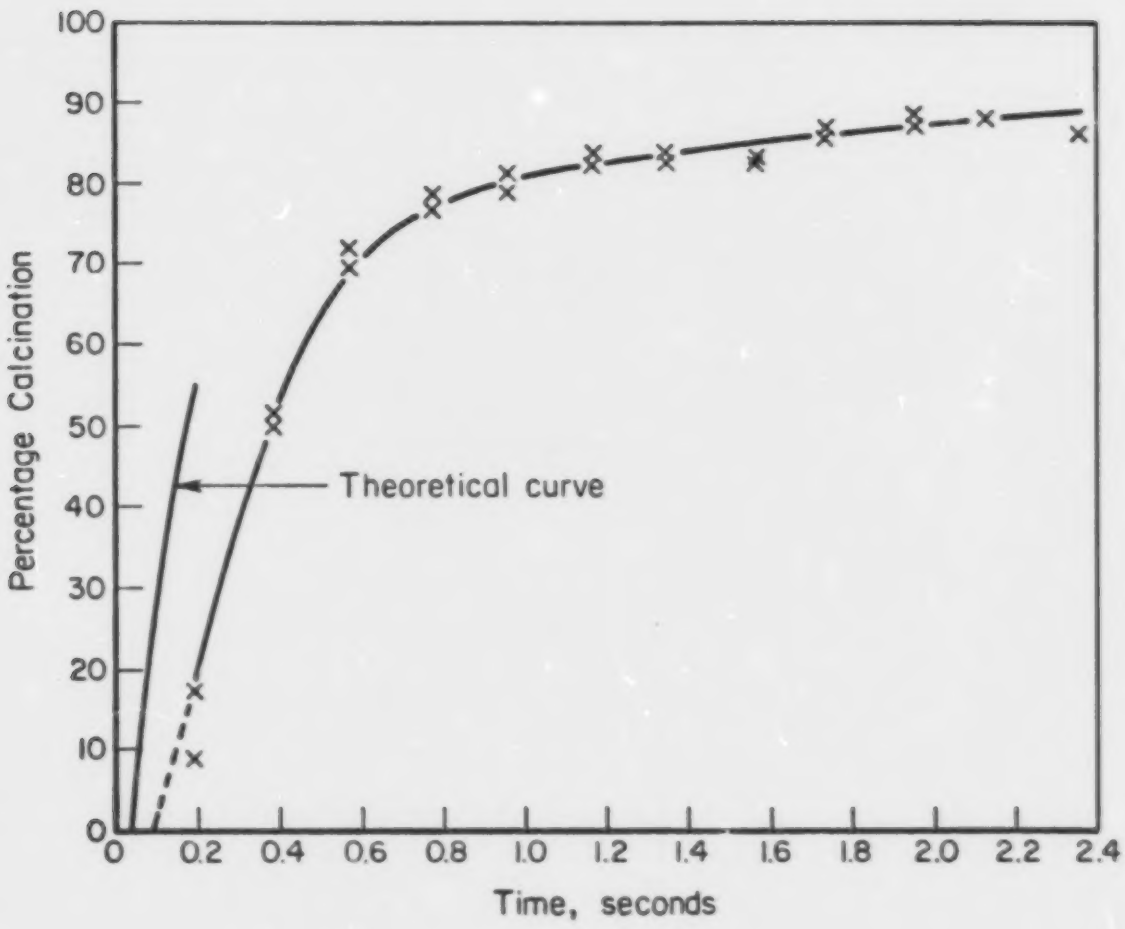

FIGURE 21. CALCINATION OF -140+200-MESH LIMESTONE AT 1863 F

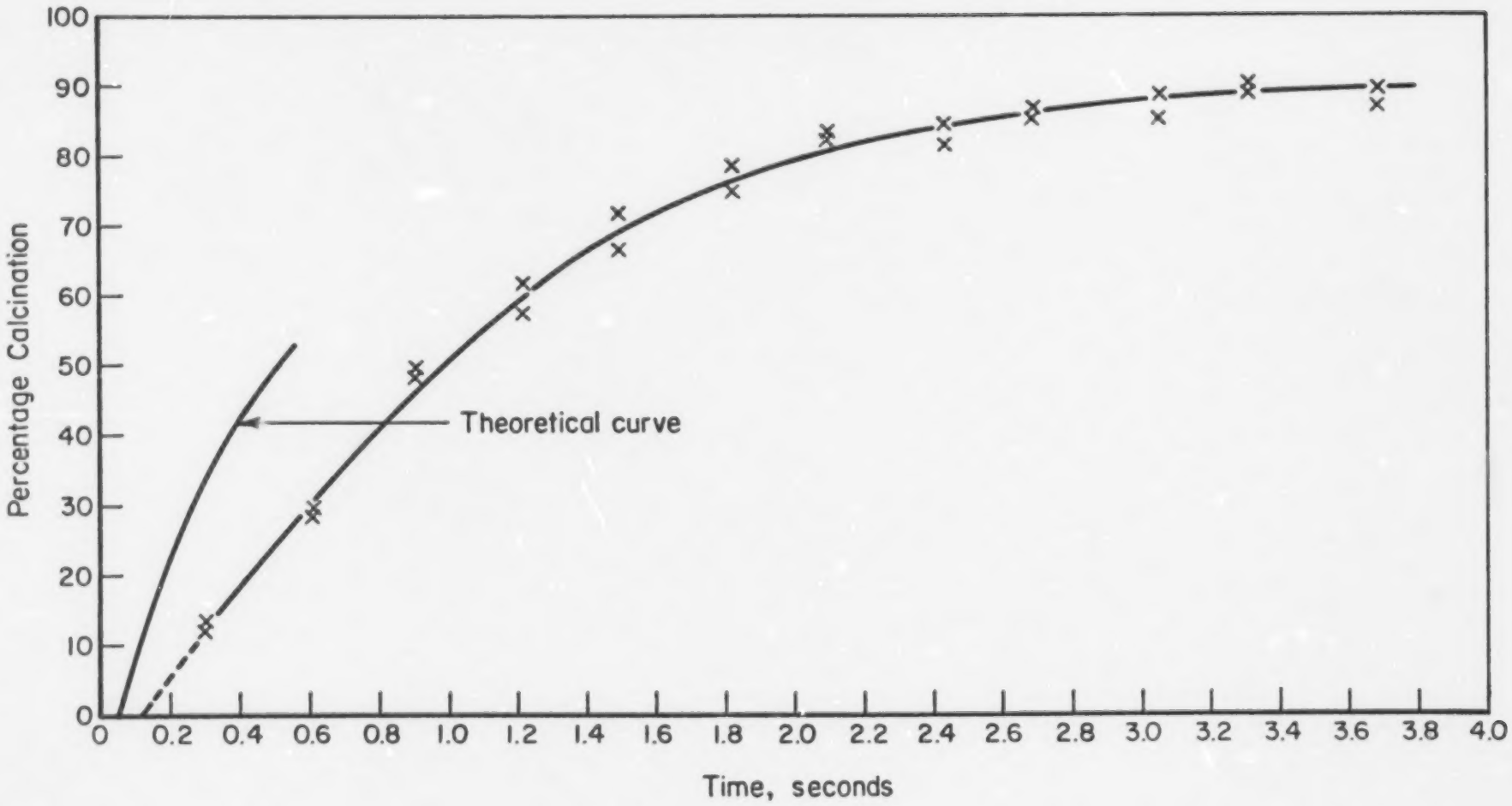

FIGURE 22. CALCINATION OF -140+200-MESH LIMESTONE AT 1600 F

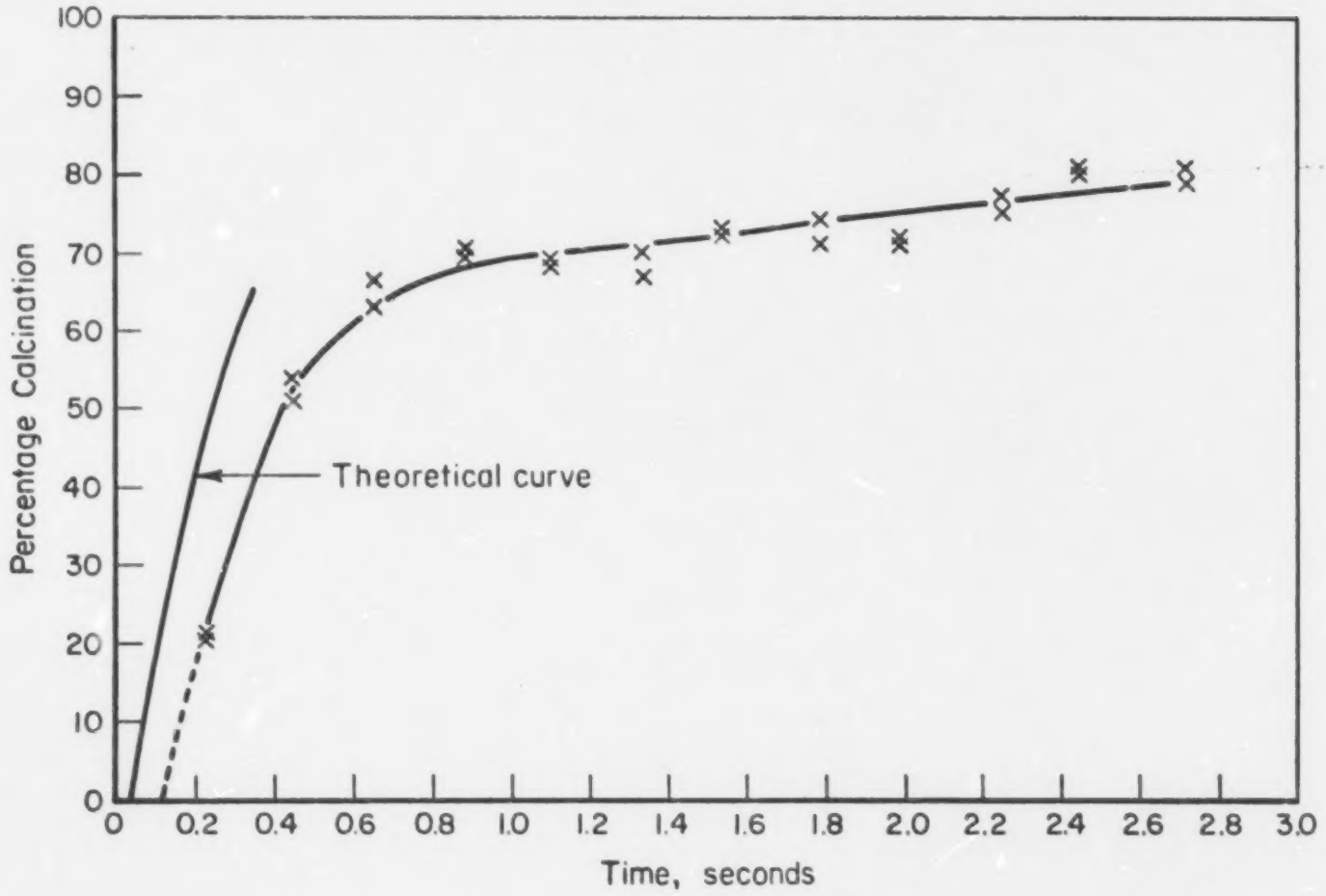

FIGURE 23. CALCINATION OF -140+200-MESH LIMESTONE AT 1770 F

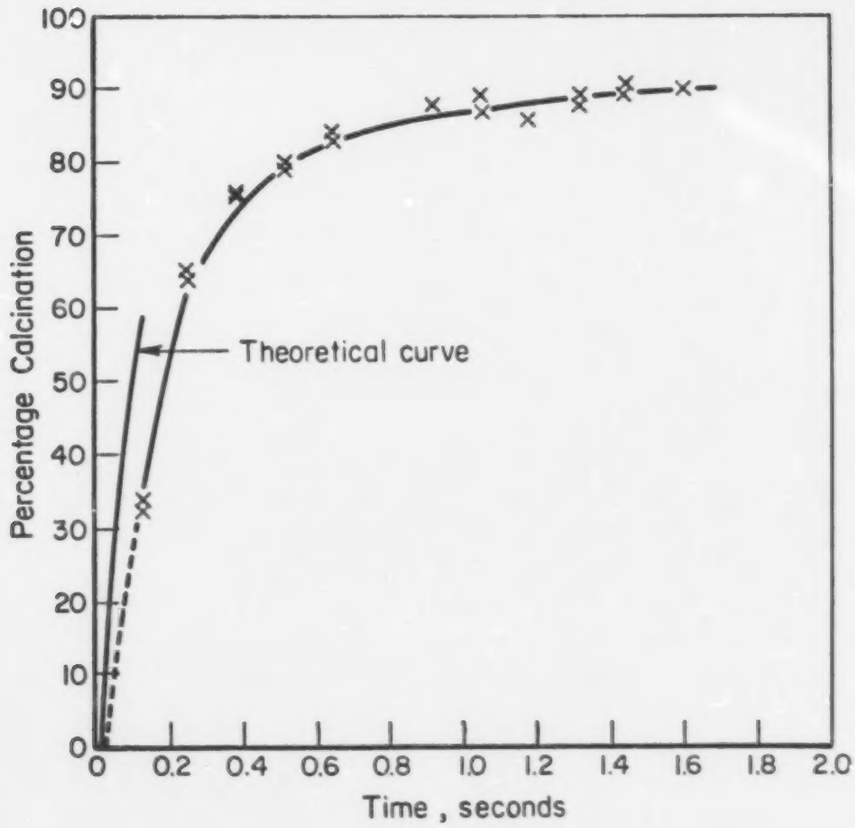

FIGURE 24. CALCINATION OF -140+200-MESH LIMESTONE AT 2068F

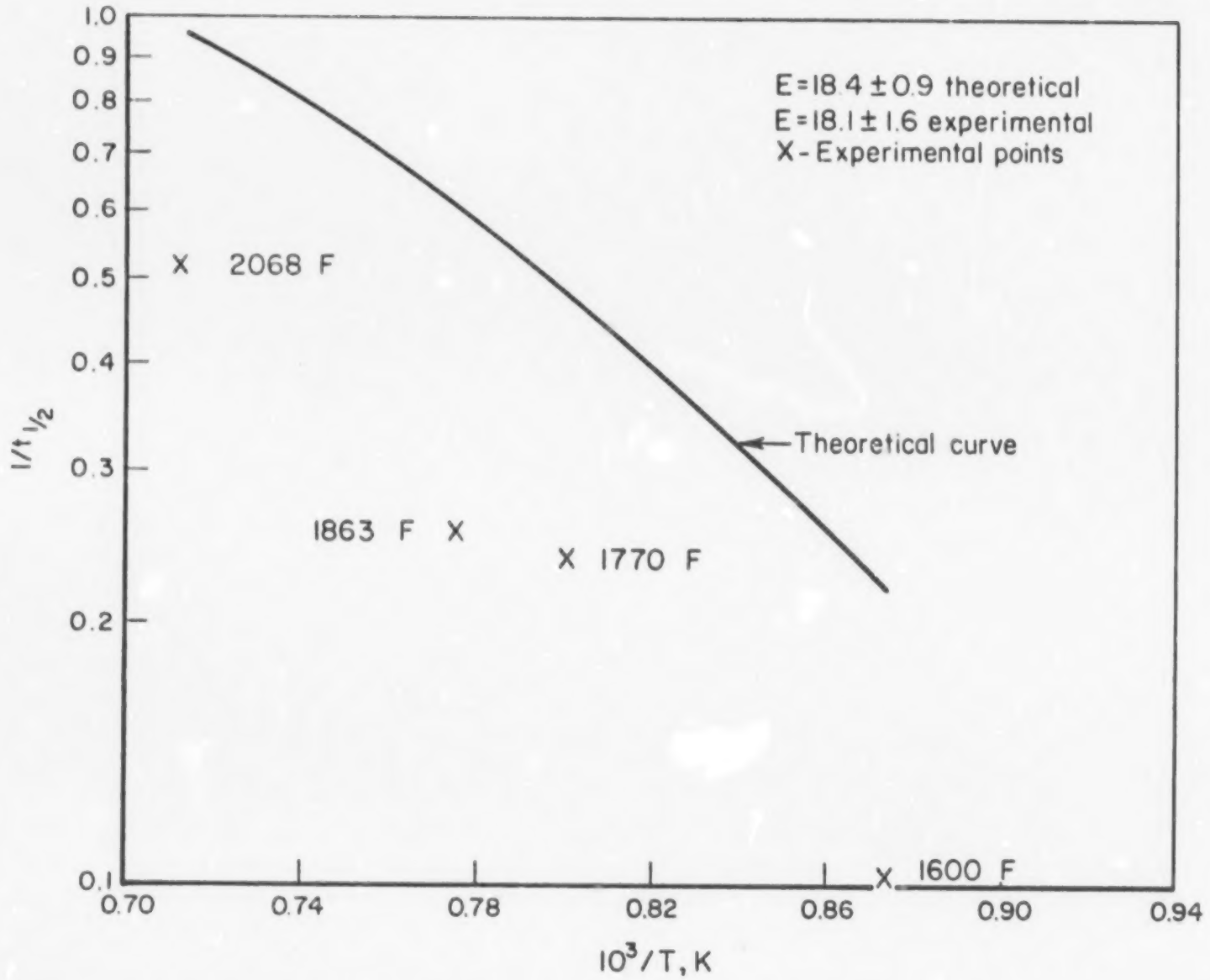

FIGURE 25. APPARENT ACTIVATION ENERGY FOR CALCINATION

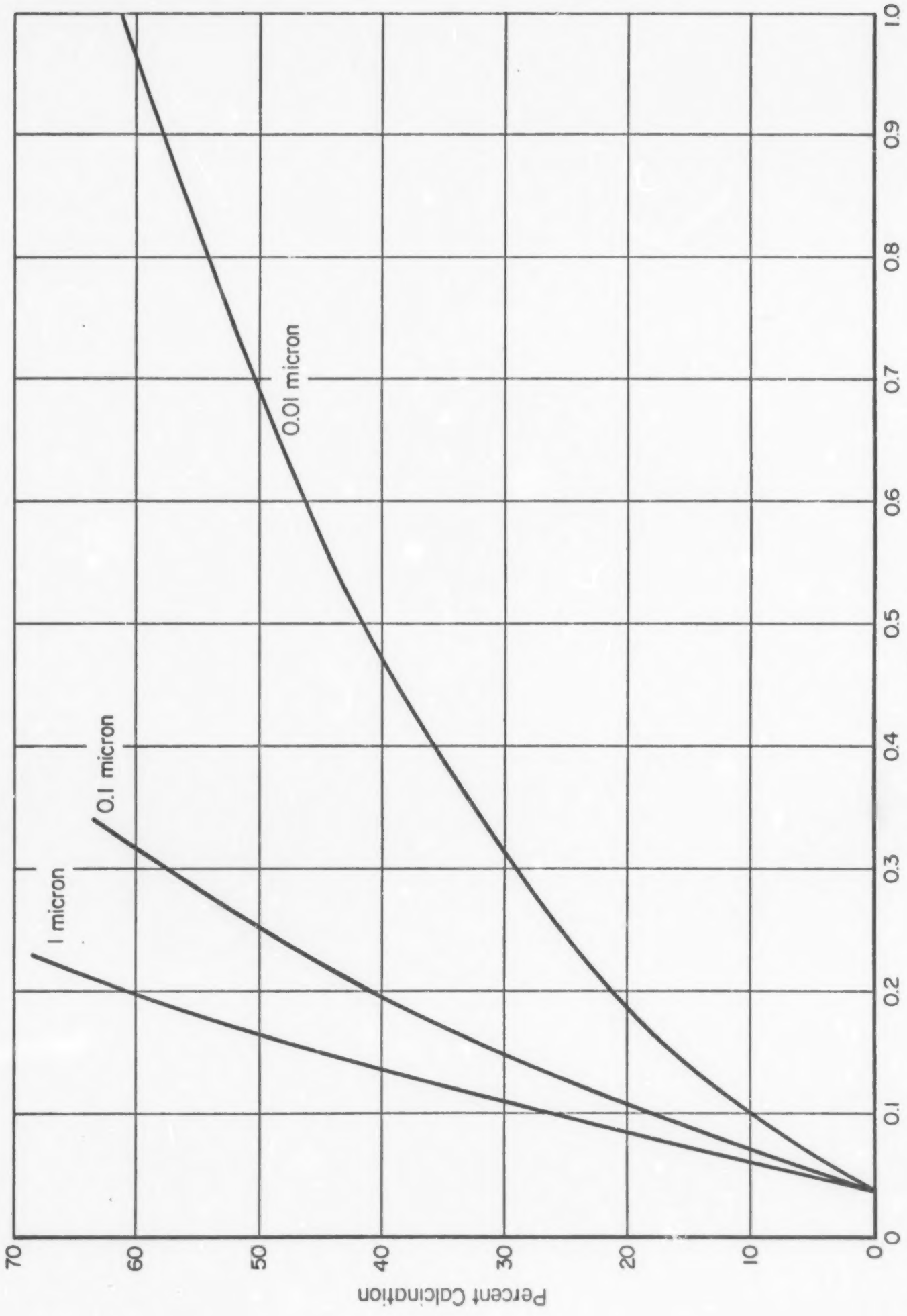

FIGURE 26. EFFECT OF PORE SIZE ON CALCINATION RATE

FUTURE WORK

This study is being continued under Contract No. CPA 70-111. The main object of the new phase of this program is to develop means for prediction of the performance of the dry-limestone-injection process in boiler furnaces on the basis of observations made using the dispersed-phase reactor. To accomplish this, modeling of the overall reaction process in terms of heat and mass transfer will be continued. Also, empirical methods will be developed for relating reactor results to boiler performance. Some additional experimental work will also be carried out to test models developed and to aid in refinement of these models. This work will include operation of the reactor under conditions such that the time-temperature profile more closely approximates that of the Shawnee boiler, on the basis of the best available information on that boiler furnace. In addition, the effects of porosity, particle size, and SO_2 concentration on the reaction rate will be determined, and these results will be incorporated as appropriate in the modeling of the overall process. Finally, some testing of the reactivity of ten stones characterized by R. Harvey (Illinois State Geological Survey) will be carried out and an attempt will be made to correlate the results with Harvey's mineralogical and petrographic data.

REFERENCES

(1) R. Coutant, et al., Summary Report on "Investigation of Reactivity of Limestone and Dolomite for Capturing SO_2 From Flue Gas" to NAPCA, June 27, 1969.

(2) R. Coutant, et al., Final Report on "Investigation of the Limestone Wet-Scrubbing Process" to NAPCA, November 30, 1969.

(3) R. Coutant, et al., Summary Report on "Investigation of the Reactivity of Limestone and Dolomite for Capturing SO_2 From Flue Gas", to NAPCA, August 30, 1968.

(4) K. H. Van Heek and H. Juntgen, "Kinetics of the Reactions of Calcium Compounds with SO_2", paper presented to the Dry Limestone Injection Process Symposium, Gilbertsville, Kentucky, June 22-26, 1970.

(5) R. Borgwardt, Environmental Science and Technology, 4, 59 (1970).

(6) C. N. Satterfield and F. Feakes, AIChE Journal, 5, 115 (1959).

(7) T. R. Ingraham and R. Marrier, Can. J. Ch.E., p 170 (August, 1963).

(8) I. Proks, Chemicke Zvesti, 20, 697 (1966).

(9) W. O. Philbrook and K. Natesen, "Mixed-Control Kinetics in the Thermal Decomposition of Calcium Carbonate", Report to National Lime Association, Washington, D. C., 1966.

(10) G. Narsimhan, Chem. Eng. Sci., 16, 7 (1961).

(11) R. T. Haslam and V. C. Smith, Ind. Eng. Chem., 20, 170 (1928).

(12) A.W.D. Hills, Chem. Eng. Sci., 23, 297 (1968).

(13) R. W. Coutant and E. H. Lougher, Monthly Letter Report on "Investigation of Reactivity of Limestone and Dolomite for Capturing SO_2 From Flue Gas" to NAPCA, April 18, 1969.

(14) W. H. McAdams, Heat Transmission, McGraw-Hill Book Co., Inc., New York (1954).

(15) A. Wheeler, Advances in Catalysis, Vol. III, (1951), p 249.

(16) R. P. Mayer and R. A. Stowe, "Physical Characterization of Limestone and Lime", Report to National Lime Association, Washington, D. C., 1964.

(17) R. H. Borgwardt, T. A. Kittleman, and R. E. Harrington, "The Dry Limestone Process for SO_2 Control: A Full Study of the Role of Over Burning", APCA Paper No. 69-141, presented at APCA Annual Meeting, New York, June 22-26, 1969.

(18) G. N. Dul'nev, J. Eng. Phys., Russian, 9, 399 (1965).

APPENDIX A

REACTOR DATA

TABLE A-1. REACTOR DATA - CALCINATION

Run	Gas Temp, F	Reynolds Number	Residence Time, sec	Product Analysis: Sample Weight, mg	Wt Loss, mg H_2O	Wt Loss, mg CO_2	Percentage Calcination
1-16-A	1604	2100	0.30	10.54	0.125	3.788	13.5
1-16-B	1604	2100	0.30	10.12	0.125	3.700	12.4
1-16-C	1604	2100	0.61	11.98	0.500	3.825	29.7
1-16-D	1604	2100	0.61	10.17	0.350	3.300	28.8
1-16-E	1604	2100	0.90	10.10	0.750	2.325	48.8
1-16-F	1604	2100	0.90	11.41	0.900	2.625	49.4
1-16-G	1604	2100	1.22	10.61	1.150	1.950	61.3
1-16-H	1604	2100	1.22	9.74	0.988	1.950	57.5
1-16-J	1604	2100	1.50	9.97	1.300	1.375	71.7
1-16-K	1604	2100	1.50	11.02	1.350	1.800	66.3
1-16-L	1604	2100	1.83	9.68	1.075	1.625	64.6
1-16-M	1604	2100	1.83	10.60	1.325	1.625	68.4
1-16-N	1604	2100	2.10	10.23	1.275	1.363	72.2
1-16-O	1604	2100	2.10	9.85	1.263	1.263	73.4
1-16P	1604	2100	2.44	9.76	1.300	1.250	73.7
1-16-Q	1604	2100	2.44	10.14	1.163	1.375	71.0
1-16-R	1604	2100	2.70	9.91	1.250	1.150	75.6
1-16-S	1604	2100	2.70	9.80	1.213	1.100	76.2
1-16-T	1604	2100	3.06	10.54	1.338	1.250	75.2
1-16-U	1604	2100	3.06	9.62	1.488	1.050	78.4
1-16-V	1604	2100	3.32	9.98	1.500	1.000	79.9
1-16-W	1604	2100	3.32	11.03	1.600	1.075	80.2
1-16-X	1604	2100	3.69	11.57	1.475	1.150	78.9
1-16-Y	1604	2100	3.69	9.54	1.300	1.050	77.4
1-20-A	1770	2400	0 22	10.28	0.275	3.475	20.6
1-20-B	1770	2400	0.22	10.14	0.250	3.425	20.3
1-20-C	1770	2400	0.45	10.38	0.638	2.138	51.4
1-20-D	1770	2400	0.45	10.45	0.750	2.100	53.9
1-20-E	1770	2400	0.66	9.81	0.838	1.600	62.9
1-20-F	1770	2400	0.66	9.95	0.750	1.375	66.3
1-20-G	1770	2400	0.89	11.17	1.175	1.550	69.6
1-20-H	1770	2400	0.89	9.97	0.850	1.300	69.1
1-20-J	1770	2400	1.10	10.01	0.800	1.300	68.5
1-20-K	1770	2400	1.10	9.98	0.775	1.300	68.1
1-20-L	1770	2400	1.34	10.67	0.825	1.300	69.7
1-20-M	1770	2400	1.34	10.68	0.763	1.400	67.0
1-20-N	1770	2400	1.54	10.05	0.913	1.150	72.9
1-20-O	1770	2400	1.54	10.38	0.950	1.200	72.8
1-20-P	1770	2400	1.79	10.46	0.800	1.200	71.1
1-20-Q	1770	2400	1.79	10.78	0.975	1.200	73.5
1-20-R	1770	2400	1.99	9.91	0.700	1.050	72.0
1-20-S	1770	2400	1.99	10.59	0.713	1.150	70.9

TABLE A-1. (Continued)

Run	Gas Temp, F	Reynolds Number	Residence Time, sec	Product Analysis: Sample Weight, mg	Wt Loss, mg H_2O	Wt Loss, mg CO_2	Percentage Calcination
1-20-T	1770	2400	2.25	10.45	1.275	1.113	77.2
1-20-U	1770	2400	2.25	10.04	1.125	1.125	75.4
1-20-V	1770	2400	2.45	10.01	1.063	0.925	78.8
1-20-W	1770	2400	2.45	10.99	1.288	0.963	80.6
1-20-X	1770	2400	2.72	10.73	1.263	1.013	79.3
1-20-Y	1770	2400	2.72	10.07	1.175	0.875	80.7
1-20-AA	1770	2400	0.22	9.96	0.275	3.425	19.7
1-20-BB	1770	2400	0.22	10.70	0.313	3.750	18.7
1-20-CC	1770	2400	0.45	11.18	0.750	2.788	44.2
1-20-DD	1770	2400	0.45	10.86	0.850	2.700	45.8
1-20-EE	1770	2400	0.66	11.85	1.425	1.850	67.5
1-20-FF	1770	2400	0.66	11.15	1.125	2.025	61.0
1-20-GG	1770	2400	0.89	11.91	1.475	1.750	69.5
1-20-HH	1770	2400	0.89	10.39	1.250	1.425	71.2
1-20-JJ	1770	2400	1.10	10.43	0.950	2.150	58.8
1-20-KK	1770	2400	1.10	9.97	1.200	1.550	67.7
1-20-LL	1770	2400	1.34	11.84	1.450	1.775	68.9
1-20-MM	1770	2400	1.34	12.00	1.525	1.600	72.4
1-20-NN	1770	2400	1.54	10.49	1.388	1.213	76.1
1-20-OO	1770	2400	1.54	10.58	1.375	1.350	73.6
1-20-PP	1770	2400	1.79	11.84	1.525	1.563	72.7
1-20-QQ	1770	2400	1.79	11.05	1.525	1.313	75.8
1-20-RR	1770	2400	1.99	10.24	1.300	1.288	73.8
1-20-SS	1770	2400	1.99	10.26	1.450	1.300	74.5
1-20-TT	1770	2400	2.25	9.69	1.350	1.100	76.9
1-20-UU	1770	2400	2.25	10.18	1.475	1.138	77.5
1-20-VV	1770	2400	2.45	10.10	1.425	1.050	78.8
1-20-WW	1770	2400	2.45	10.18	1.275	1.200	75.2
1-20-XX	1770	2400	2.72	10.38	1.413	1.163	77.0
1-20-YY	1770	2400	2.72	9.89	1.400	1.100	77.4
12-4-A	1863	2500	0.19	11.89	0.215	4.650	8.8
12-4-B	1863	2500	0.19	10.37	0.360	3.775	17.3
12-4-C	1863	2500	0.39	9.79	0.888	2.200	51.5
12-4-D	1863	2500	0.39	10.79	1.113	2.617	50.0
12-4-E	1863	2500	0.58	10.30	1.500	1.450	72.1
12-4-F	1863	2500	0.58	10.46	1.490	1.610	69.5
12-4-G	1863	2500	0.78	10.05	1.500	1.180	76.5
12-4-H	1863	2500	0.78	9.96	1.650	1.100	78.7
12-4-J	1863	2500	0.96	9.92	1.680	1.070	78.6
12-4-K	1863	2500	0.96	11.36	1.895	1.115	81.0
12-4-L	1863	2500	1.17	11.17	1.850	1.025	82.1

TABLE A-1. (Continued)

Run	Gas Temp, F	Reynolds Number	Residence Time, sec	Product Analysis: Sample Weight, mg	Wt Loss, mg H_2O	Wt Loss, mg CO_2	Percentage Calcination
12-4-M	1863	2500	1.17	10.48	1.740	0.885	83.5
12-4-N	1863	2500	1.35	10.26	1.663	0.913	82.5
12-4-O	1863	2500	1.35	10.77	1.800	0.900	83.7
12-4-P	1863	2500	1.57	10.04	1.660	0.905	82.4
12-4-Q	1863	2500	1.57	11.81	1.950	1.040	82.8
12-4-R	1863	2500	1.74	10.45	1.660	0.765	85.4
12-4-S	1863	2500	1.74	11.05	1.815	0.770	86.2
12-4-T	1863	2500	1.96	10.36	1.410	0.565	88.2
12-4-U	1863	2500	1.96	10.36	1.450	0.637	87.0
12-4-V	1863	2500	2.13	10.22	1.475	0.600	87.7
12-4-W	1863	2500	2.13	9.92	1.470	0.580	87.9
12-4-X	1863	2500	2.36	10.66	0.660	2.890	39.3
12-4-X	1863	2500	2.36	12.94	0.800	3.675	36.8
12-4-Y	1863	2500	2.36	11.07	1.735	0.790	85.7
12-5-A	2068	3100	0.13	10.94	0.670	3.365	32.1
12-5-B	2068	3100	0.13	10.28	0.725	3.160	33.2
12-5-C	2068	3100	0.26	10.88	1.427	1.875	65.2
12-5-D	2068	3100	0.26	10.14	1.360	1.840	63.6
12-5-E	2068	3100	0.39	11.25	1.790	1.410	75.5
12-5-F	2068	3100	0.39	10.11	1.515	1.270	75.1
12-5-G	2068	3100	0.53	15.24	2.400	1.550	79.9
12-5-H	2068	3100	0.53	14.59	2.300	1.550	79.1
12-5-J	2068	3100	0.66	10.22	1.725	0.910	82.7
12-5-K	2068	3100	0.66	12.51	2.050	1.025	83.9
12-5-L	2068	3100	0.80	10.42	1.690	0.870	83.6
12-5-N	2068	3100	0.92	10.09	1.610	0.605	88.0
12-5-O	2068	3100	0.92	12.15	1.940	0.750	87.6
12-5-P	2068	3100	1.06	11.43	1.815	0.635	88.8
12-5-Q	2068	3100	1.06	9.56	1.320	0.590	86.9
12-5-R	2068	3100	1.18	10.74	1.445	0.715	85.8
12-5-S	2068	3100	1.18	11.24	1.540	0.760	85.7
12-5-T	2068	3100	1.33	10.46	1.345	0.530	88.7
12-5-U	2068	3100	1.33	11.28	1.470	0.645	87.5
12-5-V	2068	3100	1.45	11.13	1.525	0.540	89.5
12-5-W	2068	3100	1.45	13.29	1.950	0.615	90.3
12-5-X	2068	3100	1.60	10.82	1.540	0.520	89.8
12-5-Y	2068	3100	1.60	10.85	1.770	0.715	86.9

TABLE A-2. REACTOR DATA - SULFURIZATION

Run Number	Gas Temp, °F	Reynolds Number	Residence Time, sec	Product Analysis					CaO Utilization, Percent	mg SO_3 Per Gram Calcine	Percentage Calcination	Gas Analysis, Volume Percent		
				Weight, mg	Total* Sulfur	* Sulfate	CO_2 mg	H_2O mg				SO_2	CO_2	O_2
2-5-C	1600	2000	0.65	10.04	2.5	0.9	3.350	0.450	1.42	18.3	24.2	0.303	10.0	3.0
2-5-F	1600	2000	0.96	10.07	9.4	5.7	2.275	0.900	5.13	66.1	50.8	0.303	10.0	3.0
2-5-G	1600	2000	1.30	10.00	6.2	5.7	1.650	1.150	3.43	44.2	65.3	0.303	10.0	3.0
2-5-K	1600	2000	1.60	10.02	13.3	12.1	0.950	1.325	7.53	97.0	80.1	0.303	10.0	3.0
2-5-L	1600	2000	1.95	9.98	13.0	11.8	0.850	1.450	7.02	90.5	82.5	0.303	10.0	3.0
2-5-O	1600	2000	2.24	10.07	17.3	15.3	0.500	1.638	8.99	116	90.0	0.303	10.0	3.0
2-5-P	1600	2000	2.60	9.97	17.0	14.4	0.525	1.663	8.64	111	89.4	0.303	10.0	3.0
2-5-S	1600	2000	2.88	10.01	19.0	17.6	0.175	1.650	10.36	134	96.4	0.303	10.0	3.0
2-5-T	1600	2000	3.24	10.00	19.4	17.2	0.225	1.700	10.18	131	95.5	0.303	10.0	3.0
2-5-W	1600	2000	3.51	10.09	22.0	19.8	0.200	1.675	11.65	150	96.0	0.303	10.0	3.0
2-18-A	1691	2100	0.26	10.05	3.4	1.4	3.775	0.113	2.11	27.2	10.2	0.296	10.0	3.0
2-18-B	1691	2100	0.26	10.11	2.3	3.7	3.850	0.150	1.39	17.9	9.4	0.296	10.0	3.0
2-18-C	1691	2100	0.53	10.09	5.6	2.4	2.813	0.525	3.41	43.9	36.6	0.296	10.0	3.0
2-18-E	1691	2100	0.78	10.07	9.4	6.7	1.575	1.175	5.16	66.5	67.1	0.296	10.0	3.0
2-18-H	1691	2100	1.05	10.00	11.0	7.9	1.200	1.313	6.00	77.3	75.1	0.296	10.0	3.0
2-18-K	1691	2100	1.29	10.14	14.0	11.3	0.700	1.550	7.48	96.6	85.7	0.296	10.0	3.0
2-18-L	1691	2100	1.57	10.11	14.7	13.5	0.600	1.400	8.64	111	87.5	0.296	10.0	3.0
2-18-N	1691	2100	1.81	10.08	17.7	16.6	0.350	1.550	9.93	128	92.8	0.296	10.0	3.0
2-18-Q	1691	2100	2.10	10.14	20.1	15.3	0.250	1.600	11.13	143	94.9	0.296	10.0	3.0
2-18-S	1691	2100	2.33	10.05	20.4	18.3	0.400	1.400	12.1	155	91.6	0.296	10.0	3.0
2-18-T	1691	2100	2.62	9.96	20.5	19.4	0.250	1.475	11.9	154	94.7	0.296	10.0	3.0
2-18-V	1691	2100	2.84	10.05	23.4	20.9	0.400	1.288	14.5	187	91.3	0.296	10.0	3.0
2-18-Y	1691	2100	3.14	10.02	21.8	19.8	0.430	1.450	12.3	159	91.1	0.296	10.0	3.0

* Expressed as weight percent $CaSO_4 \cdot 2H_2O$.

TABLE A-2. REACTOR DATA - SULFURIZATION (Continued)

Run Number	Gas Temp, °F	Reynolds Number	Residence Time sec	Product Analysis					CaO Utilization, Percent	mg SO_3 Per Gram Calcine	Percentage Calcination	Gas Analysis, Volume Percent		
				Weight, mg	Total Sulfur	Sulfate	CO_2 mg	H_2O mg				SO_2	CO_2	O_2
3-25-B	1692	1900	0.30	10.00	2.9	2.0	3.675	0.225	1.73	22.2	14.5	0.301	10.4	3.0
3-25-C	1692	1900	0.61	10.11	4.5	2.9	2.850	0.650	2.55	32.9	37.4	0.301	10.4	3.0
3-25-F	1692	1900	0.91	9.94	9.6	6.5	1.300	1.250	5.31	68.4	71.7	0.301	10.4	3.0
3-25-H	1692	1900	1.23	10.00	11.0	8.6	1.100	1.338	6.05	78	76.4	0.301	10.4	3.0
3-25-J	1692	1900	1.80	10.00	15.8	13.3	0.338	1.600	8.69	112	93.1	0.301	10.4	3.0
3-25-L	1692	1900	2.13	10.02	16.5	16.1	0.250	1.650	8.99	116	94.9	0.301	10.4	3.0
3-25-O	1692	1900	2.47	10.03	18.4	15.8	0.250	1.575	10.3	133	94.9	0.301	10.4	3.0
3-25-Q	1692	1900	2.74	10.00	20.3	18.6	0.313	1.550	11.2	145	93.6	0.301	10.4	3.0
3-25-R	1692	1900	3.09	10.01	21.0	19.6	0.225	1.550	11.8	152	95.3	0.301	10.4	3.0
3-25-T	1692	1900	3.35	9.93	21.8	21.7	0.138	1.550	12.4	159	97.1	0.301	10.4	3.0
3-25-W	1692	1900	3.71	10.00	24.1	21.4	0.225	1.500	13.7	176	95.3	0.301	10.4	3.0
2-17-A	1845	2700	0.18	10.06	5.0	2.9	3.500	0.250	0.42	17.4	18.2	0.277	10.0	3.0
2-17-B	1845	2700	0.18	10.11	4.0	3.0	3.525	0.300	0.25	12.4	18.6	0.277	10.0	3.0
2-17-D	1845	2700	0.36	10.00	7.3	4.7	2.100	0.868	4.24	54.6	54.2	0.277	10.0	3.0
2-17-F	1845	2700	0.53	10.10	8.6	5.6	1.250	1.263	4.87	62.8	74.2	0.277	10.0	3.0
2-17-G	1845	2700	0.72	10.05	11.3	9.0	0.575	1.600	6.08	78.4	88.5	0.277	10.0	3.0
2-17-K	1845	2700	0.89	10.00	10.8	8.8	0.375	1.725	5.66	72.9	92.3	0.277	10.0	3.0
2-17-M	1845	2700	1.08	9.99	14.8	12.0	0.337	1.750	7.57	97.6	93.2	0.277	10.0	3.0
2-17-O	1845	2700	1.25	10.02	14.5	11.3	0.362	1.650	7.80	100	92.4	0.277	10.0	3.0
2-17-P	1845	2700	1.44	10.07	17.8	16.4	0.300	1.675	9.42	121	93.8	0.277	10.0	3.0
2-17-S	1845	2700	1.60	10.18	18.1	15.8	0.362	1.625	9.78	126	92.5	0.277	10.0	3.0
2-17-U	1845	2700	1.80	10.02	18.9	17.2	0.162	1.675	10.2	131	96.9	0.277	10.0	3.0
2-17-W	1845	2700	0.18	10.15	7.9	3.8	3.325	0.313	4.77	61.5	22.6	0.277	10.0	3.0

TABLE A-2. REACTOR DATA - SULFURIZATION (Continued)

Run Number	Gas Temp, °F	Reynolds Number	Residence Time, sec	Product Analysis: Weight, mg	Total Sulfur	Sulfate	CO_2 mg	H_2O mg	CaO Utilization, Percent	mg SO_3 Per Gram Calcine	Percentage Calcination	Gas Analysis, volume percent: SO_2	CO_2	O_2
2-3-A	2041	3200	0.13	10.04	5.2	2.5	3.775	0.200	3.04	39.1	14.2	0.305	10.2	3.0
2-3-B	2041	3200	0.13	10.34	14.7	1.9	3.887	0.200	8.16	105	18.4	0.305	10.2	3.0
2-3-C	2041	3200	0.26	10.05	4.1	3.0	2.850	0.663	2.30	29.7	37.1	0.305	10.2	3.0
2-3-D	2041	3200	0.26	10.20	7.4	5.2	1.825	1.100	4.10	52.9	62.1	0.305	10.2	3.0
2-3-E	2041	3200	0.39	9.68	15.1	6.3	1.750	1.063	7.92	102	61.5	0.305	10.2	3.0
2-3-F	2041	3200	0.39	9.91	18.5	5.3	1.500	1.100	10.1	130	67.7	0.305	10.2	3.0
2-3-G	2041	3200	0.52	10.33	7.5	6.6	1.080	1.480	4.05	52.2	78.7	0.305	10.2	3.0
2-3-H	2041	3200	0.52	9.78	9.8	7.0	1.250	1.275	5.32	68.5	73.5	0.305	10.2	3.0
2-3-J	2041	3200	0.64	10.15	9.5	4.8	0.950	1.500	5.07	65.3	81.1	0.305	10.2	3.0
2-3-K	2041	3200	0.64	10.03	9.3	9.0	1.050	1.450	4.94	63.6	78.7	0.305	10.2	3.0
2-3-L	2041	3200	0.78	10.61	10.8	9.8	0.980	1.630	5.58	71.8	81.4	0.305	10.2	3.0
2-3-O	2041	3200	0.90	10.54	11.1	9.0	0.800	1.680	5.75	74.1	84.8	0.305	10.2	3.0
2-3-P	2041	3200	1.04	11.80	12.0	11.0	0.930	1.850	6.23	80.3	84.1	0.305	10.2	3.0
2-3-Q	2041	3200	1.16	10.02	13.7	10.5	0.625	1.600	7.19	92.6	87.4	0.305	10.2	3.0
2-19-B	2109	3600	0.11	10.03	4.5	3.7	3.050	0.325	2.92	37.6	28.5	0.302	10.0	3.0
2-19-D	2109	3600	0.22	10.04	6.7	5.3	1.200	1.450	3.50	45.1	75.6	0.302	10.0	3.0
2-19-E	2109	3600	0.33	10.12	6.4	5.0	1.762	1.175	3.44	44.4	63.4	0.302	10.0	3.0
2-19-G	2109	3600	0.44	9.98	7.7	7.5	0.362	1.800	3.97	51.1	92.7	0.302	10.0	3.0
2-19-K	2109	3600	0.54	10.12	7.9	6.7	0.675	1.675	4.10	52.8	86.4	0.302	10.0	3.0
2-19-M	2109	3600	0.65	10.02	7.6	7.4	0.200	1.912	3.85	49.6	96.1	0.302	10.0	3.0
2-19-N	2109	3600	0.75	9.99	7.7	5.2	0.700	1.600	4.09	52.7	85.4	0.302	10.0	3.0
2-19-P	2109	3600	0.87	10.06	8.5	8.3	0.150	1.950	4.26	54.9	97.1	0.302	10.0	3.0
2-19-S	2109	3600	0.97	5.74	6.1	5.7	0.587	0.800	3.40	43.8	78.9	0.302	10.0	3.0
2-19-U	2109	3600	1.09	10.02	9.5	9.2	0.150	1.900	4.83	62.3	97.0	0.302	10.0	3.0
2-19-V	2109	3600	1.19	10.07	8.3	7.1	0.550	1.713	4.32	55.7	88.9	0.302	10.0	3.0
2-19-X	2109	3600	1.31	10.00	9.7	9.5	0.250	1.800	5.07	65.3	94.9	0.302	10.0	3.0

TABLE A-2. REACTOR DATA - SULFURIZATION (Continued)

Run Number	Gas Temp, °F	Reynolds Number	Residence Time, sec	Product Analysis					CaO Utilization, Percent	mg SO_3 Per Gram Calcine	Percentage Calcination	Gas Analysis, Volume Percent		
				Weight, mg	Total Sulfur	Sulfate	CO_2 mg	H_2O mg				SO_2	CO_2	O_2
3-26-B	2148	3600	0.10	10.00	11.3	8.4	2.100	0.763	6.79	87.5	53.1	0.306	10.4	2.6
3-26-C	2148	3600	0.21	10.01	12.5	6.5	0.963	1.375	6.88	88.6	80.2	0.306	10.4	2.6
3-26-F	2148	3600	0.31	10.07	6.4	5.0	0.550	1.700	3.39	43.6	89.2	0.306	10.4	2.6
3-26-H	2148	3600	0.42	10.09	6.1	5.9	0.338	1.900	3.06	39.5	93.5	0.306	10.4	2.6
3-26-J	2148	3600	0.62	10.06	5.7	5.4	0.200	1.950	2.87	37.0	96.2	0.306	10.4	2.6
3-26-L	2148	3600	0.73	10.00	6.7	6.1	0.200	1.950	3.34	43.0	96.2	0.306	10.4	2.6
3-26-N	2148	3600	0.84	10.08	3.3	2.8	0.325	1.775	1.79	23.0	93.6	0.306	10.4	2.6
3-26-Q	2148	3600	0.94	10.05	6.9	6.1	0.200	1.850	3.62	46.6	96.1	0.306	10.4	2.6
3-26-R	2148	3600	1.05	10.08	8.1	23.5	0.150	1.950	4.08	52.5	97.1	0.306	10.4	2.6
3-26-U	2148	3600	1.15	10.02	6.9	6.4	0.325	1.850	3.52	45.3	93.6	0.306	10.4	2.6
3-26-W	2148	3600	1.27	10.08	8.0	7.2	0.200	1.900	4.08	52.6	96.2	0.306	10.4	2.6
4-17-BB	1690	2200	0.26	10.00	4.1	2.9	3.530	0.250	2.47	31.8	17.1	0.748	10.0	3.0
4-17-CC	1690	2200	0.53	9.99	7.0	3.1	2.500	0.725	4.02	51.8	44.7	0.748	10.0	3.0
4-17-EE	1690	2200	0.79	10.06	12.6	10.1	1.280	1.250	6.96	89.6	73.3	0.738	10.0	3.0
4-17-HH	1690	2200	1.06	10.02	14.8	10.0	0.825	1.400	8.20	106	83.0	0.748	10.0	3.0
4-17-KK	1690	2200	1.31	10.07	17.7	15.4	0.375	1.550	9.87	127	92.3	0.748	10.0	3.0
4-17-LL	1690	2200	1.59	10.02	21.7	17.1	0.275	1.500	12.4	159	94.3	0.748	10.0	3.0
4-17-NN	1690	2200	1.84	9.97	23.2	21.5	0.225	1.530	13.0	167	95.3	0.748	10.0	3.0
4-17-QQ	1690	2200	2.13	9.96	25.5	21.0	0.300	1.500	14.1	181	93.7	0.748	10.0	3.0
4-17-SS	1690	2200	2.37	10.07	27.6	25.9	0.175	1.530	15.4	198	96.3	0.748	10.0	3.0
4-17-TT	1690	2200	2.67	10.08	28.8	25.8	0.150	1.450	16.7	216	96.8	0.748	10.0	3.0
4-17-VV	1690	2200	2.91	10.09	31.4	29.8	0.150	1.480	17.7	22.8	96.8	0.748	10.0	3.0
4-17-YY	1690	2200	3.22	10.01	32.3	30.5	0.163	1.430	18.4	238	96.5	0.748	10.0	3.0

TABLE A-2. REACTOR DATA - SULFURIZATION (Continued)

Run Number	Gas Temp, F	Reynolds Number	Residence Time, sec	Product Analysis					CaO Utilization, Percent	mg SO_3 Per Gram Calcine	Percentage Calcination	Gas Analysis, Volume Percent		
				Weight, mg	Total Sulfur	Sulfate	CO_2 mg	H_2O mg				SO_2	CO_2	O_2
4-17-B	1703	2200	0.26	9.99	3.5	2.6	3.500	0.288	2.08	26.8	18.3	0.954	9.8	3.0
4-17-C	1703	2200	0.53	9.94	7.6	4.7	2.330	0.775	4.37	56.4	48.4	0.954	9.8	3.0
4-17-E	1703	2200	0.78	10.04	13.3	9.1	0.960	1.300	7.63	98.2	79.9	0.954	9.8	3.0
4-17-H	1703	2200	1.05	9.98	13.8	12.1	0.760	1.390	7.81	100	84.2	0.954	9.8	3.0
4-17-K	1703	2200	1.30	10.07	20.0	18.9	0.400	1.500	11.2	145	91.7	0.954	9.8	3.0
4-17-L	1703	2200	1.58	9.99	21.4	19.6	0.300	1.460	12.4	160	93.7	0.954	9.8	3.0
4-17-N	1703	2200	1.82	9.97	26.9	24.4	0.200	1.450	15.5	200	95.7	0.954	9.8	3.0
4-17-Q	1703	2200	2.11	9.98	27.5	26.1	0.300	1.430	15.6	201	93.6	0.954	9.8	3.0
4-17-S	1703	2200	2.34	10.05	35.5	29.4	0.180	1.430	19.9	256	96.1	0.954	9.8	3.0
4-17-T	1703	2200	2.64	10.04	31.7	30.3	0.200	1.450	17.9	230	95.7	0.954	9.8	3.0
4-17-V	1703	2200	2.87	10.05	34.5	32.7	0.213	1.350	20.2	260	95.4	0.954	9.8	3.0
4-17-Y	1703	2200	3.18	9.98	36.6	34.7	0.138	1.350	21.4	275	97.3	0.954	9.8	3.0
4-16-BB	1692	2000	0.28	10.03	2.1	1.3	3.650	0.200	1.29	16.6	14.3	0.04	10.0	3.0
4-16-CC	1692	2000	0.57	10.01	2.6	2.3	2.550	0.700	1.54	19.8	43.6	0.04	10.0	3.0
4-16-EE	1692	2000	0.84	9.94	3.6	2.5	1.550	1.200	2.00	25.8	67.6	0.04	10.0	3.0
4-16-HH	1692	2000	1.14	10.04	5.1	4.5	1.100	1.400	2.81	36.3	77.6	0.04	10.0	3.0
4-16-KK	1692	2000	1.40	10.03	4.5	3.4	0.900	1.600	2.34	30.2	82.2	0.04	10.0	3.0
4-16-LL	1692	2000	1.70	10.01	5.0	4.3	0.700	1.550	2.77	35.7	85.9	0.04	10.0	3.0
4-16-NN	1692	2000	1.96	10.00	6.7	4.7	0.480	1.750	3.48	44.8	90.6	0.04	10.0	3.0
4-16-QQ	1692	2000	2.27	9.93	6.1	6.0	0.600	1.700	3.16	40.7	88.1	0.04	10.0	3.0
4-16-SS	1692	2000	2.52	10.09	6.4	4.9	0.440	1.790	3.32	42.7	91.5	0.04	10.0	3.0
4-16-TT	1692	2000	2.84	9.98	6.9	6.2	0.440	1.750	3.60	46.4	91.4	0.04	10.0	3.0
4-16-VV	1692	2000	3.08	10.08	6.5	4.5	0.350	1.830	3.36	43.3	93.3	0.04	10.0	3.0
4-16-YY	1692	2000	3.41	10.02	7.0	6.3	0.380	1.750	3.71	47.8	92.6	0.04	10.0	3.0

TABLE A-2. REACTOR DATA - SULFURIZATION (Continued)

Run Number	Gas Temp, °F	Reynolds Number	Residence Time, sec	Product Analysis					CaO Utilization, Percent	mg SO_3 Per Gram Calcine	Percentage Calcination	Gas Analysis, Volume Percent		
				Weight, mg	Total Sulfur	Sulfate	CO_2 mg	H_2O mg				SO_2	CO_2	O_2
4-16-B	1717	2600	0.21	9.97	2.4	1.9	3.780	0.150	1.45	18.7	10.0	0.300	8.0	6.0
4-16-C	1717	2600	0.42	10.10	4.9	3.0	2.850	0.600	2.85	36.7	36.7	0.300	8.0	6.0
4-16-E	1717	2600	0.62	10.01	7.4	6.9	1.700	1.100	4.14	53.3	64.0	0.300	8.0	6.0
4-16-H	1717	2600	0.84	10.11	9.5	7.8	1.150	1.350	5.23	67.4	76.5	0.300	8.0	6.0
4-16-K	1717	2600	1.04	10.07	11.6	10.5	0.740	1.500	6.35	81.8	85.0	0.300	8.0	6.0
4-16-N	1717	2600	1.45	10.06	15.7	13.7	0.330	1.650	8.48	109	93.4	0.300	8.0	6.0
4-16-Q	1717	2600	1.68	10.02	16.8	14.7	0.350	1.600	9.18	118	92.9	0.300	8.0	6.0
4-16-S	1717	2600	1.87	9.99	19.2	18.4	0.330	1.600	10.4	134	93.2	0.300	8.0	6.0
4-16-T	1717	2600	2.10	10.00	19.8	17.2	0.280	1.650	10.5	135	94.3	0.300	8.0	6.0
4-16-V	1717	2600	2.28	9.97	21.3	18.9	0.260	1.590	11.6	149	94.6	0.300	8.0	6.0
4-16-Y	1717	2600	2.51	10.06	20.7	18.7	0.250	1.600	11.4	146	94.9	0.300	8.0	6.0
4-15-B	1711	1800	0.31	10.06	4.0	1.6	3.380	0.380	2.33	30.1	22.7	0.301	11.6	0.4
4-15-D	1711	1800	0.62	9.99	4.9	3.7	2.300	0.840	2.80	36.0	50.0	0.301	11.6	0.4
4-15-E	1711	1800	0.91	10.09	8.0	5.2	1.450	1.150	4.62	59.5	69.6	0.301	11.6	0.4
4-15-H	1711	1800	1.24	10.00	6.9	4.8	1.000	1.460	3.72	47.9	79.8	0.301	11.6	0.4
4-15-K	1711	1800	1.52	10.08	9.3	6.2	0.340	1.750	4.94	63.6	93.4	0.301	11.6	0.4
4-15-L	1711	1800	1.86	10.02	9.2	7.0	300	1.710	5.00	64.4	94.1	0.301	11.6	0.4
4-15-N	1711	1800	2.13	10.00	11.1	8.2	0.300	1.780	5.75	74.1	94.1	0.301	11.6	0.4
4-15-Q	1711	1800	2.48	10.09	13.8	11.0	0.290	1.730	7.31	94.1	94.3	0.301	11.6	0.4
4-15-S	1711	1800	2.75	10.04	14.8	12.7	0.230	1.750	7.78	100	95.4	0.301	11.6	0.4
4-15-T	1711	1800	3.11	10.03	14.1	13.0	0.190	1.710	7.65	99	96.2	0.301	11.6	0.4
4-15-V	1711	1800	3.37	10.02	14.5	12.0	0.200	1.750	7.66	99	96.0	0.301	11.6	0.4
4-15-Y	1711	1800	3.74	10.00	15.4	13.6	0.190	1.700	8.02	103	96.2	0.301	11.6	0.4

TABLE A-2. REACTOR DATA - SULFURIZATION (Continued)

Run Number	Gas Temp °F	Reynolds Number	Residence Time, Sec	Product Analysis					CaO Utilization, Percent	mg SO_3 Per Gram Calcine	Percentage Calcination	Gas Analysis, Volume Percent		
				Weight, mg	Total Sulfur	Sulfate	CO_2 mg	H_2O mg				SO_2	CO_2	O_2
4-10-B	1945	2600	0.17	10.03	7.6	4.7	1.300	1.180	4.45	57.4	70.3	0.306	10.0	3.0
4-10-C	1945	2600	0.35	9.97	8.7	6.5	0.550	1.550	4.87	62.7	88.8	0.306	10.0	3.0
4-10-E	1945	2600	0.52	10.01	9.5	8.5	0.250	1.730	5.15	66.4	95.1	0.306	10.0	3.0
4-10-H	1945	2600	0.70	10.05	9.8	8.9	0.150	1.830	5.17	66.6	97.1	0.306	10.0	3.0
4-10-K	1945	2600	0.86	10.05	10.8	8.9	0.250	1.780	5.69	73.3	95.1	0.306	10.0	3.0
4-10-L	1945	2600	1.05	9.97	11.6	10.8	0.150	1.800	6.11	78.7	97.0	0.306	10.0	3.0
4-10-N	1945	2600	1.21	10.10	13.6	11.8	0.150	1.750	7.35	94.7	97.0	0.306	10.0	3.0
4-10-Q	1945	2600	1.40	9.96	13.6	12.1	0.138	1.750	7.27	93.7	97.2	0.306	10.0	3.0
4-10-S	1945	2600	1.56	10.08	15.3	13.4	0.100	1.750	8.27	107	98.0	0.306	10.0	3.0
4-10-T	1945	2600	1.75	9.98	14.1	13.9	0.100	1.780	7.48	96.4	98.0	0.306	10.0	3.0
4-10-V	1945	2600	1.90	10.10	13.8	13.6	0.113	1.780	7.40	95.3	97.8	0.306	10.0	3.0
4-10-Y	1945	2600	2.10	10.03	14.7	14.2	0.100	1.750	7.93	102	98.0	0.306	10.0	3.0
4-9-B	1717	1800	0.30	10.09	6.5	3.5	1.600	1.100	3.76	48.5	64.1	0.305	10.0	3.0
4-9-C	1717	1800	0.61	9.97	8.1	5.5	0.975	1.380	4.54	58.4	78.6	0.305	10.0	3.0
4-9-E	1717	1800	0.90	10.04	9.2	7.4	0.575	1.600	5.00	64.5	88.5	0.305	10.0	3.0
4-9-H	1717	1800	1.22	9.95	11.4	10.0	0.500	1.550	6.34	81.6	89.8	0.305	10.0	3.0
4-9-K	1717	1800	1.51	10.09	11.3	10.1	0.313	1.700	6.13	78.9	93.8	0.305	10.0	3.0
4-9-M	1717	1800	1.84	10.09	16.6	11.2	0.300	1.730	8.64	111	94.1	0.305	10.0	3.0
4-9-N	1717	1800	2.12	10.07	14.5	12.4	0.200	1.780	7.58	97.7	96.1	0.305	10.0	3.0
4-9-Q	1717	1800	2.46	10.01	15.7	13.6	0.250	1.750	8.16	105	95.0	0.305	10.0	3.0
4-9-S	1717	1800	2.73	10.02	16.2	15.3	0.200	1.730	8.57	110	96.0	0.305	10.0	3.0
4-9-T	1717	1800	3.08	9.99	18.9	15.9	0.250	1.650	10.1	130	94.9	0.305	10.0	3.0
4-9-V	1717	1800	3.34	10.04	18.7	17.1	0.150	1.700	10.0	129	97.0	0.305	10.0	3.0
4-9-Y	1717	1800	3.70	9.94	19.4	18.1	0.113	1.650	10.6	137	97.7	0.305	10.0	3.0

APPEN X B

COMPUTER PROGRAM - SULFEX

PROCESSING OF ANALYTICAL DATA

APPENDIX B

COMPUTER PROGRAM - SULFEX

PROCESSING OF ANALYTICAL DATA

SULFEX

```
010 DIMENSION X1(24),X2(24),Y1(24),Y2(24),SWT(24),IDENT(24)
020 INPUT,N
021 INPUT3000,DATE,(IDENT(I),I=1,N)
022 INPUT,(SWT(I),I=1,N)
030 INPUT,(Y1(I),I=1,N),(Y2(I),I=1,N)
040 INPUT,(X1(I),I=1,N),(X2(I),I=1,N)
045 PRINT 500,DATE
050 PRINT 1000
060 CC1=145./172. ; CC2=120./172. ; CC3=74./18.
070 CC4=100./44. ; CC5=56./145. ; CC6=56./120.
080 CC7=56./74 ; CC8=0.56 ; CC9=80./145.
090 CC10=80./120. ; CC11=89./145. ; CC12=64./120.
110 DO 10 I=1,N
120 A=Y2(I)*SWT(I)*CC1/100.
130 B=(Y1(I)-Y2(I))*SWT(I)*CC2/100.
140 C=X2(I)*CC3
150 D=X1(I)*CC4
160 G=(A*CC5+B*CC6+C*CC7+D*CC8)*.10904
170 ACC=(A+B+C+D+G)/SWT(I)
180 SRAT=1.0-Y2(I)/Y1(I)
190 UTAP=(A*CC5+B*CC6)*10.904/G
200 UTRE=100.*(A*CC5+B*CC6)/(A*CC5+B*CC6+C*CC7)
210 SPMG=1000.*(A*CC9+B*CC10)/G/10.17
220 CALA=UTAP+10.904*C*CC7/G
230 E=SWT(I)-G-D-A*CC11-B*CC12-C/CC3
240 CALB=100.*E/(E+D*CC8)
250 CALAV=(CALA+CALB)/2.0
255 PRINT 4000,IDENT(I)
260 PRINT 2000,SWT(I),Y1(I),Y2(I),X1(I),X2(I),SRAT,UTAP,
270 & UTRE,SPMG,CALA,CALB, CALAV,ACC
280 10 CONTINUE
310 STOP
315 500 FORMAT(1H0,A4)
320 1000 FORMAT("0 SWT  TSULF SATE CO2  H2O  SRAT UTAP UTRE SPMG"
330 &,"  CALA  CALB  CALAV ACC",/)
350 2000 FORMAT(1X,3F5.2,3(1X,F4.2)2F5.2,4F6.2,F5.2)
360 4000 FORMAT(1X,A1)
370 3000 FORMAT(A4,1X,24(A1,1X))
400 END
```

APPENDIX C

COMPUTER PROGRAM - DRH2
DATA CORRELATION

APPENDIX C

COMPUTER PROGRAM - DRH2

DATA CORRELATION

DRH2

```
100 DIMENSION S(4,25),EL1(4,25),EL2(4,25),EN(4),A(4),B(4)
110 DIMENSION SF(100),Y(100),D(4),X(100),NS(4),TM(4),C(4)
120 PRINT 6000
130 INPUT,NSET
140 PRINT 5000
150 K=1
160 DO 3 I=1,NSET
170 INPUT, NS(I),TM(I),C(I)
180 PRINT 5001
190 N=NS(I)
200 INPUT,(S(I,J),EL1(I,J),EL2(I,J), J=1,N)
210 DO 2 J=1,N
220 X(K)=S(I,J)
230 2 K=K+1
240 3 CONTINUE
250 4 M=1
260 PRINT 5002
270 5 INPUT, (B(I), I=1,4)
280 10 BT=B(M)
290 KK=1
300 DO 67 I=1,NSET
310 NN=NS(I)
320 DO 15 J=1,NN
330 CALL TRAP (BT,TM(I),EL1(I,J),EL2(I,J),SX)
340 SF(KK)=C(I)*SX
350 15 KK=KK+1
360 67 CONTINUE
370 KK=KK-1
380 CALL FIT(SF,X,SLO,YINT,KK)
390 EN(M)=SLO-1.
400 A(M) = EXP(-YINT)/SLO
410 SD2=0.
420 DO 120 I=1,KK
430 ST =(ABS(A(M)*SLO*SF(I)))**(1./SLO)
440 120 SD2 = SD2+(X(I)-ST)**2
450 P=KK-2
460 D(M)=SQRT(SD2/P)
470 M=M+1
480 IF(M.LE.4) GO TO 10
490 PRINT 1000,(B(I),EN(I),A(I),D(I),I=1,4)
500 16 PRINT 5003
510 INPUT,IFLAG
520 IF(IFLAG) 99,25,4
530 25 PRINT 5004
540 INPUT,K
550 PRINT 5005,B(K)
560 PRINT 5010
570 INPUT,I
580 PRINT 5011
590 PRINT 5011,TM(I)
```

DRH2 CONTINUED

```
600 SD2=0.0
610 NN=NS(I)
620 DO 30 J=1,NN
630 CALL TRAP(B(K),TM(I),EL1(I,J),EL2(I,J),SX)
640 30 SF(J)=C(I)*SX
650 PRINT 2000
660 DO 40 J=1,NN
670 ST=(ABS(A(K)*(EN(K)+1.)*SF(J)))**(1./(EN(K)+1))
680 T=C(I)*(EL2(I,J)-EL1(I,J))
690 PRINT 3000,S(I,J),ST,T
700 40 SD2=SD2+(S(I,J)-ST)**2
710 P=NS(I)-2
720 DEV= SQRT(SD2/P)
730 PRINT 4000, DEV
740 GO TO 16
750 99 STOP
760 1000 FORMAT(7X,1HB,13X,1HN,13X,1HA,8X,5HDEV-S/(4E14.7)//)
770 2000 FORMAT(7X,1HS,13X,1HS,13X,1HT,/4X,7H(INPUT),8X,5H(CAL) )
780 3000 FORMAT(3E14.7)
790 4000 FORMAT(" STANDARD DEVIATION OF S - ",E14.7)
800 5000 FORMAT(" NS,TM,C"/)
810 5001 FORMAT(" S,L1,L2"/)
820 5002 FORMAT(" B"/)
830 5003 FORMAT(" FLAG; -1=STOP, 0=FINAL B, 1=NEW SET OF B"/)
840  5004 FORMAT(" USE B(I) FROM ABOVE;  I =  ")
850 5005 FORMAT(/" B = ",E14.7)
860 5010 FORMAT(" SET NUMBER  ")
870 5011 FORMAT(" TM(J) = ",E14.7//)
880 6000 FORMAT(" NUMBER OF DATA SETS  ")
890 END
900 SUBROUTINE TRAP(B,TM,EL1,EL2,SX)
910 EXFUNC(X)=EXP(-B/((TM-32.)*5./9.+273.+27.8*(6.-X)))
920 N=(EL2-EL1)/.01-1.
930 SUM=EXFUNC(EL1)/2. + EXFUNC(EL2)/2.
940 DO 10 I=1,N
950 X=EL1+.01*I
960 10 SUM=SUM+EXFUNC(X)
970 SX=.01*SUM
980 RETURN
990 END
1000 SUBROUTINE FIT(Y,X,EM,B,NN)
1010 DIMENSION AM(2,2),Y1(100),NS(1),X1(100)
1020 DIMENSION Y(100),X(100),PHI(100,2),A(2),RW(200)
1030 DO 10 I=1,NN
1040 Y1(I)=ALOG(ABS(Y(I)))
1050 X1(I)=ALOG(ABS(X(I)))
1060 PHI(I,1)=1.0
1070 10 PHI(I,2)=X1(I)
1080 NS(1)=NN
1090 N=2
```

DRH2 CONTINUED

```
1100 M=NN
1110 CALL LSQMM(PHI,Y1,A,RW,M,N,NT,NS,AM,100,2)
1120 EM=A(2)
1130 B=A(1)
1140 RETURN
1150 END
```

APPENDIX D

COMPUTER PROGRAM - CALCIN

CALCINATION MODEL

APPENDIX D

CALCIN

```
100 REAL NRE,L,K,M,MC
110 DIMENSION Y(101),YY(101),YYY(101),GRY(101),GR2Y(101),YDOT(101)
120 DIMENSION YDOT1(101),R(101),D(101),P(101),GRP(101),JCOUNT(11)
130 DIMENSION GR2YP(101),GR2YPP(101)
140 FUNCD(TF,PF)=2./3.*A*SQRT(8*RGASC*(TF+460.)/M/3.1416*3.22E05)
150 & +A^2/ETA*PF*3.22E05
160 FUNCTC(PF)=(40.4E03/1.987/(24.195-ALOG(PF))-273.)*1.8+32.
170 FUNCTG(PF)=40.4E03/1.987*1.8/(24.195-ALOG(PF))^2/PF
180 FUNCSG(TF)=.156+.194E-03*TF-.056E-06*TF^2
190 FUNCTD(IH,GR,GRGR)=K/S1/RHO1*(GRGR+2*GR/R(IH)-RGF*GR/K*
200 & FUNCSG(Y(N+3-IH))*(RC/R(IH))^2)
210 FUNCH(T1,T2)=HKG*(.015+.7E-05*(T1+T2))+EPS*SIG*(T1+T2+920.)
220 & *((T1+460.)^2+(T2+460.)^2)
230 FUNCGP(TH,DH,RH)=RGASC/M*RGF*(TH+460.)/DH*(RC/RH)^2
240 NRE=.06; S2=.2; RHO2=169.; S1=.2; RHO1=95.; TO=70.; EPS=.3
250 SIG=.173E-08; M=44.;MC=100.;L=710.;ETA=.1;RGASC=555.
260 5 PRINT 7
270 7 FORMAT(" TG,PG,RO,A,K,ENDCAL,FRAC,IND")
280 INPUT, TG,PG,RO,A,THK,ENDCAL,FRAC,IND
290 DATA N,EGP,EGR,EGS/50,.00001,.001,.001/
300 K=THK; TC=FUNCTC(PG)
310 HKG=.5/RO (2.+.37*NRE^.6)
320 H=FUNCH(TC,TG)
330 DELT=S2*RHO2*RO/3/H*ALOG((TG-TO)/(TG-TC))/20
340 DELTAR=RO/N; TIME=0.; TCO=TC; PCT=10.
350 PC=PG; PC1=PC; PCP=PC
360 ICALC=0; JCALC=0; N1=N+1; N2=N+2
370 DO 10 I=1,N1
380 YDOT1(I)=0.; YYY(I)=0.; P(I)=PG
390 10 R(I)=(I-1)*DELTAR
400 JCOUNT(1)=N1; ICOUNT=1
410 DO 20 I=1,N
420 IF (100*(1.-(R(N1-I)/RO)^3)-ICOUNT*PCT) 20,15,15
430 15 JCOUNT(ICOUNT+1)=N2-I
440 ICOUNT=ICOUNT+1
450 20 CONTINUE
460 Y(2)=TO; TDOT1=0.
470 30 H=FUNCH(Y(2),TG)
480 TDOT2=H*(TG-Y(2))*3/RO/S2/RHO2
490 IF (TDOT1) 35,33,35
500 33 TDOT1=TDOT2
510 35 Y(2)=Y(2)+DELT/2*(3*TDOT2-TDOT1)
520 TIME=TIME+DELT; TDOT1=TDOT2
530 IF (Y(2)-TC) 40,50,50
540 40 TP=Y(2)
550 GO TO 30
560 50 TIME=TIME-DELT*(Y(2)-TC)/(Y(2)-TP)
570 Y(1)=RO; JEX=N+1; J=N; NJ=0; NJ2=2
580 Y(2)=TC; TIMEX=TIME; RCDOT1=0.
590 YY(2)=TC; RCDOT=0.; RC=RO
```

CALCIN CONTINUED

```
600 H=FUNCH(TC,TG)
610 GRC=H/K*(TG-TC)/(1.+M/MC*FUNCSC(TC)/L*(TG-TC))
620 NJ=N-J; NJ2=NJ+2; NO=0
630 DELT=0.
640 PRINT," TIME  CALC      R         T      P         D"
650 DC=FUNCD(TC,PC)
660 250 CALC=100*(1.-(RC/RO)^3)
670 IF (CALC-95.) 255,395,395
680 255 IF (ICALC-1) 280,270,275
690 270 IF (CALC-PCT) 260,272,272
700 272 TIMINT=TIME-TIMEX; GO TO 280
710 275 IF (TIME-TIMEX-ICALC*TIMINT) 260,280,280
720 280 ICALC=ICALC+1
730 PRINT 300, 3600*TIME,CALC,RC/RO,TC,PC,DC
740 300 FORMAT(F7.4,F6.1,F7.3,F9.2,F7.1,F9.5)
750 305 IF (J-JEX) 310,320,320
760 310 JEX=J
770 JCALC=1+IFIX(CALC/PCT)
780 320 IF (RC-RO) 335,260,260
790 335 DO 345 I=1,JCALC
800 IQ=JCOUNT(JCALC-I+1)
810 PRINT 340, R(IQ)/RO, Y(N+3-IQ), P(IQ),D(IQ)
820 345 CONTINUE
830 340 FORMAT(13X,F7.3,F9.2,F7.1,F9.5)
840 130 IF (CALC-ENDCAL) 260,390,390
850 260 NC=0; ITR=1; ITS=1; TIME=TIME+DELT
860 IF (RC-RO) 350,65,396
870 350 IF (RC-R(J)) 360,360,500
880 360 J=J-1; NJ=N-J; NJ2=NJ+2
890 DQ=R(J+1)-RC
900 GR2Y(NJ2)=GR2C+DQ/DELTAR*(GR2Y(NJ+1)-GR2C)
910 GRY(NJ2)=GRC+DQ/2*(GR2Y(NJ2)+GR2C)
920 Y(NJ2)=TC+DQ/2*(GRY(NJ2)+GRC)
930 GR2YPP(NJ2)=GR2Y(NJ2)-(GR2Y(NJ+1)-GR2YPP(NJ+1))
940 500 GRCP=GRC; GRC=2*GRCP-GRC1; GRC1=GRCP
950 PCP=PC; PC=2*PCP-PC1; PC1=PCP
960 Y(1)=RC; RCDOT1=RCDOT
970 DO 510 I=2,NJ2
980 II=NJ+4-I; YYY(II)=YY(II); YY(II)=Y(II)
990 GR2YP(II)=GR2Y(II); GR2Y(II)=2*GR2YP(II)-GR2YPP(II)
1000 510 GR2YPP(II)=GR2YP(II)
1010 65 TC=FUNCTC(PC); DTCDP=FUNCTG(PC)
1020 C1=RC/3./L*RHO2*S2*DTCDP*RGASC*(TC+460.)/DC/MC
1030 85 C2=K*GRC/L/RHO2
1040 THD1=K/RHO1/S1; THDG=K/RHO2/FUNCSG(TC)*MC/M
1050 THDE=THD1*THDG/(THD1+THDG)
1060 IF (C1*C2-.001) 90,95,95
1070 90 RCDOT=-C2*(1.-C1*C2*(1.-2*C1*C2)); GO TO 97
1080 95 RCDOT=.5/C1-SQRT((.5/C1)^2+C2/C1)
1090 97 RGF=-M/MC*RHO2*RCDOT
```

CALCIN CONTINUED

```
1100 DC=FUNCD(TC,PC)
1110 GRPC=FUNCGP(TC,DC,RC)
1120 TCDOT=3.*L/RC/S2*C1*RCDOT^2
1130 GR2C=TCDOT/THD1-GRC*(2./RC+RCDOT/THDE)
1140 IF (RC-RO) 103,102,396
1150 102 H=FUNCH(TC,TG)-RGF*FUNCSG(.5*(TC+TG))
1160 CALL COMP(ITS,INT,H/K*(TG-TC)/GRC,EGS,GRC,1.)
1170 GRC1=GRC
1180 GO TO (85,120,391), INT
1190 120 IF (DELT) 125,125,103
1200 125 DELT=-FRAC*DELTAR/RCDOT
1210 TIME=TIME+DELT
1220 103 IF (RCDOT1) 99,98,99
1230 98 DR=-RCDOT*DELT; GR2Y(NJ2)=GR2C
1240 GR2YPP(NJ2)=GR2C; RCDOT1=RCDOT
1250 RC=Y(1)-DR; GO TO 100
1260 99 RC=Y(1)+.5*(RCDOT+RCDOT1)*DELT
1270 DR=R(J+1)-RC
1280 100 GRY(NJ+2)=GRC+DR/2*(GR2C+GR2Y(NJ+2))
1290 Y(NJ+2)=TC+DR/2*(GRC+GRY(NJ+2))
1300 D(J+1)=FUNCD(Y(NJ+2),P(J+1))
1310 GRP(J+1)=FUNCGP(Y(NJ+2),D(J+1),R(J+1))
1320 ICHK=0
1330 110 IF (NJ-1) 402,405,405
1340 402 PRC=P(N1)+DR/2*(GRPC+GRP(N1))
1350 GO TO 427
1360 405 DO 425 I=1,NJ
1370 GRY(NJ2-I)=GRY(NJ+3-I)+DELTAR/2*(GR2Y(NJ+3-I)+GR2Y(NJ2-I))
1380 Y(NJ2-I)=Y(NJ+3-I)+DELTAR/2*(GRY(NJ+3-I)+GRY(NJ2-I))
1390 D(J+1+I)=FUNCD(Y(NJ+2-I),P(J+1+I))
1400 GRP(J+1+I)=FUNCGP(Y(NJ+2-I),D(J+1+I),R(J+1+I))
1410 425 CONTINUE
1420 DO 426 I=1,NJ
1430 426 P(N1-I)=P(N2-I)+DELTAR/2*(GRP(N2-I)+GRP(N1-I))
1440 PRC=P(J+1)+DR/2*(GRPC+GRP(J+1))
1450 427 IF (ABS(PRC/PC-1.)-EGP) 429,429,428
1460 428 PC=PRC; GO TO 65
1470 429 PC=PRC; TC=FUNCTC(PC)
1480 430 H=FUNCH(Y(2),TG)-RGF*FUNCSG(.5*(Y(2)+TG))*(RC/RO)^2
1490 CALL COMP(ITS,INT,H/K*(TG-Y(2))/GRY(2),EGS,GRC,.25)
1500 GO TO (480,490,391),INT
1510 480 NC=NC+1
1520 IF (NC-40) 65,394,394
1530 490 GRY(NJ2)=GRC+DR/2*(GR2C+GR2Y(NJ2))
1540 Y(NJ2)=TC+DR/2*(GRC+GRY(NJ2))
1550 YDOT(NJ2)=FUNCTD(J+1,GRY(NJ2),GR2Y(NJ2))
1560 IF (YYY(NJ2)) 603,605,603
1570 603 YDOT1(NJ2)=(3*Y(NJ2)-4*YY(NJ2)+YYY(NJ2))/2/DELT
1580 CALL COMP(ITR,INT,YDOT(NJ2)/YDOT1(NJ2),EGR,GR2Y(NJ2),.25)
1590 GO TO (495,605,392),INT
```

CALCIN CONTINUED

```
1600 495 ICHK=ICHK+1; GO TO 490
1610 605 IF (NJ-1) 610,606,606
1620 606 DO 520 I=1,NJ
1630 410 GRY(NJ2-I)=GRY(NJ+3-I)+DELTAR/2*(GR2Y(NJ+3-I)+GR2Y(NJ2-I))
1640 Y(NJ2-I)=Y(NJ+3-1)+DELTAR/2*(GRY(NJ+3-I)+GRY(NJ2-I))
1650 YDOT(NJ2-I)=FUNCTD(J+1+I,GRY(NJ2-I),GR2Y(NJ2-I))
1660 YDOT1(NJ2-I)=(3*Y(NJ2-I)-4*YY(NJ2-I)+YYY(NJ2-I))/2/DELT
1670 CALL COMP(ITR,INT,YDOT(NJ2-I)/YDOT1(NJ2-I),EGR,GR2Y(NJ2-I),.25)
1680 GO TO (497,520,393), INT
1690 497 ICHK=ICHK+1; GO TO 410
1700 520 CONTINUE
1710 610 IF (ICHK-1) 250,100,100
1720 396 PRINT," RC=",RC; GO TO 395
1730 391 PRINT," C3>.25,GRC,J=",J; GO TO 395
1740 392 PRINT," C3>.25, ZONE 1, J=", J; GO TO 395
1750 393 PRINT," C3>.25, I=", I, " J=", J; GO TO 395
1760 394 PRINT," NC LIMIT EXCEEDED, J=",J
1770 395 PRINT 300, 3600*TIME,CALC,Y(1)/RO,TC,PC,DC
1780 390 GO TO (5,400), IND
1790 400 STOP
1800 END
1810 SUBROUTINE COMP(IT,IN,RT,ER,VAR,AL)
1820 IF (ABS(RT-1.)-ER) 90,90,10
1830 10 IF (IT-2) 20,30,40
1840 20 RT1=RT; IT=2; IN=1
1850 VAR=VAR*(1.+AL*(RT1-1.)); GO TO 100
1860 30 RT2=RT; IT=3; IN=1
1870 VAR=VAR*(1.-AL*(RT1-1.))/(1.+AL*(RT1-1.)); GO TO 100
1880 40 RT3=RT; IT=1
1890 C=2*(RT2+RT3-2*RT1)*(RT1-1.)/(RT2-RT3)^2
1900 IF (C-.25) 60,60,50
1910 50 IN=3; VAR=VAR/(1.-AL*(RT1-1.)); GO TO 100
1920 60 IN=1
1930 IF (C-.005) 70,70,80
1940 70 VAR=VAR*(1.-AL*2*(RT1-1.)^2/(RT2-RT3)*(1.+C*(1.+2*C)))/
1950 & (1.-AL*(RT1-1.)); GO TO 100
1960 80 VAR=VAR*(1.+AL*(RT2-RT3)/2/(RT2+RT3-2*RT1)*(RT1-1.)*
1970 & (-1.+SQRT(1.-4*C)))/(1.-AL*(RT1-1.)); GO TO 100
1980 90 IN=2; IT=1
1990 100 RETURN
2000 END
```